

Titanocene Borane σ -Complexes

Clare N. Muhoro, Xiaoming He, and John F. Hartwig*

Contribution from the Department of Chemistry, Yale University, P.O. Box 208107, New Haven, Connecticut 06520-8107

Received January 8, 1999

Abstract: The chemistry of titanocene bisborane complexes $\text{Cp}_2\text{Ti}(\text{HBcat}')_2$ (**1a–g**) ($\text{HBcat}' = \text{catecholborane}$ or a substituted catecholborane) and monoborane complexes $\text{Cp}_2\text{Ti}(\text{HBcat}')(\text{L})$ (**2–4**) ($\text{L} = \text{PMe}_3$, PhSiH_3 , or PhCCPh) is reported. These complexes are unusual σ -complexes. The B–H bond in the catecholborane of **1** acts as a two-electron-donor ligand. The 4-*tert*-butyl version **1a** was studied in depth and underwent ligand substitution reactions with PMe_3 , CO, PhSiH_3 , and PhCCPh . The products of the reaction of **1a** with PMe_3 and PhSiH_3 are the novel monoborane σ -complexes $\text{Cp}_2\text{Ti}(\text{HBcat}')(\text{PMe}_3)$ (**2a**; $\text{HBcat}' = \text{HBO}_2\text{C}_6\text{H}_3\text{-4-}t\text{-Bu}$) and $\text{Cp}_2\text{Ti}(\text{HBcat}')(\text{PhSiH}_3)$ (**3**; $\text{HBcat}' = \text{HBO}_2\text{C}_6\text{H}_3\text{-4-}t\text{-Bu}$), in which the catecholborane remains a two-electron-donating ligand. Reaction with CO formed $\text{Cp}_2\text{Ti}(\text{CO})_2$. Reaction with PhCCPh formed $\text{Cp}_2\text{Ti}(\text{HBcat}')(\text{PhCCPh})$ (**4**; $\text{HBcat}' = \text{HBO}_2\text{C}_6\text{H}_3\text{-4-}t\text{-Bu}$), which was observed in solution and reductively eliminated the vinyl boronate ester $(\text{Ph})(\text{Bcat}')\text{C}=\text{C}(\text{Ph})(\text{H})$. The rates for the reactions of **1a** with these substrates showed a first-order dependence on the concentration of **1a** and a zero-order dependence on the concentrations of both the departing HBcat' and the incoming ligand. The substitution reaction proceeded at the same rate $((3.8 \pm 0.3) \times 10^{-4})$ regardless of the identity of the incoming ligand. The entropy of activation was $+30 \pm 5$ eu. These data are consistent with a dissociative substitution mechanism for the reaction of **1a** with these substrates. The ΔH^\ddagger value of 25 ± 3 kcal mol $^{-1}$ for these reactions provides an upper limit for the strength of the borane–metal interaction. Electronic effects on the reaction rate support a bonding model involving back-donation from titanium to the borane, and the unusual steric effects allow a proposal for the geometric changes that occur upon formation of the transition state.

Introduction

Transition metal σ -complexes are a remarkable type of coordination complex created by intermolecular binding of a substrate to a metal center through an X–H σ -bond. Stable σ -complexes are limited to examples where X is H or Si, and numerous examples of dihydrogen and silane complexes have been reported.^{1–3} Transition metal alkane σ -complexes are highly unstable,⁴ but have been detected in the gas phase,⁵ in matrix isolation,^{6,7} in solution by direct NMR spectroscopic observation of continuously irradiated solutions⁸ or by indirect mechanistic probes such as isotopic labeling and kinetic isotope effects,^{9–12} and in the solid state when supported by accompanying hydrophobic interactions.¹³ The intramolecular

variants of alkane σ -complexes are commonly referred to as agostic complexes. These complexes are generally more stable because the X–H donor possesses another point of attachment to the metal, and many examples of agostic complexes are known.¹⁴

σ -Complexes have been invoked as intermediates in the oxidative addition of X–H bonds to transition metals. These addition reactions are important because they provide the initial step for activation of unreactive substrates. This enhancement of reactivity by coordination of the X–H σ -bond is an important step in catalytic hydrogenation^{15,16} and hydrosilylation^{16–18} and for stoichiometric processes such as C–H activation^{19–23} and σ -bond metatheses.^{24,25} α -Agostic interactions in metal alkyl

- (1) Crabtree, R. H. *Angew. Chem., Int. Ed. Engl.* **1993**, *32*, 789.
- (2) Heinekey, D. M.; Oldham, W. J. *Chem. Rev.* **1993**, *93*, 913.
- (3) Schubert, U. *Adv. Organomet. Chem.* **1990**, *30*, 151.
- (4) For a review of transition metal alkane complexes see: Hall, C.; Perutz, R. N. *Chem. Rev.* **1996**, *96*, 3125.
- (5) Brown, C. E.; Ishikawa, Y.-I.; Hackett, P. A.; Rayner, D. M. *J. Am. Chem. Soc.* **1990**, *112*, 2530.
- (6) Turner, J. J.; Burdett, J. K.; Perutz, R. N.; Poliakov, M. *Pure Appl. Chem.* **1977**, *49*, 271.
- (7) Rest, A. J.; Whitwell, I.; Graham, W. A. G.; Hoyano, J. K.; McMaster, A. D. *J. Chem. Soc.* **1987**, 1181.
- (8) Geftakis, S.; Ball, G. E. *J. Am. Chem. Soc.* **1998**, *120*, 9953.
- (9) Buchanan, J. M.; Stryker, J. M.; Bergman, R. G. *J. Am. Chem. Soc.* **1986**, *108*, 1537–1550.
- (10) Gould, G. L.; Heinekey, D. M. *J. Am. Chem. Soc.* **1989**, *111*, 5502.
- (11) Bullock, R. M.; Headford, C. E. L.; Hennessy, K. M.; Kegley, S. E.; Norton, J. R. *J. Am. Chem. Soc.* **1989**, *111*, 3897.
- (12) Bullock, R. M. In *Transition Metal Hydrides*; Dedieu, A., Ed.; VCH: New York, 1992; p 263.
- (13) Evans, D. R.; Drovetskaya, T.; Bau, R.; Reed, C. A.; Boyd, P. D. *W. J. Am. Chem. Soc.* **1997**, *119*, 3633.

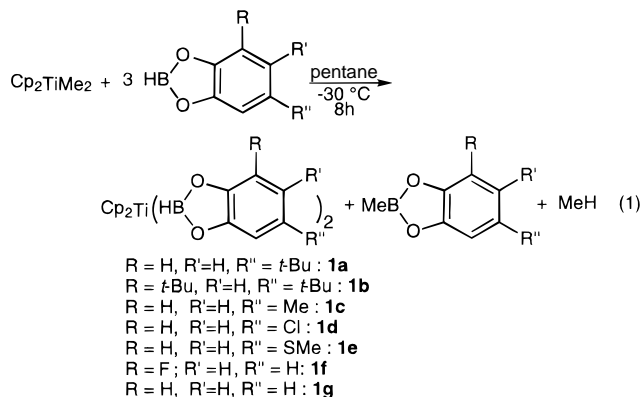
- (14) Brookhart, M.; Green, M. L. H.; Wong, L.-L. *Prog. Inorg. Chem.* **1988**, *36*, 1–124.
- (15) Halpern, J. *Science* **1982**, *217*, 401.
- (16) Collman, J. P.; Hegedus, L. S.; Norton, J. R.; Finke, R. G. *Principles and Applications of Organotransition Metal Chemistry*, 2nd ed.; University Science Books: Mill Valley, CA, 1987.
- (17) Chalk, A. J.; Harrod, J. F. *J. Am. Chem. Soc.* **1965**, *87*, 16.
- (18) Sommer, L. H.; Lyons, J. E.; Fujimoto, H. *J. Am. Chem. Soc.* **1969**, *91*, 2670.
- (19) Crabtree, R. H. *Chem. Rev.* **1995**, *95*, 987.
- (20) Hill, C. L. *Activation and Functionalization of Alkanes*; John Wiley and Sons: New York, 1989.
- (21) Arndtsen, B. A.; Bergman, R. G.; Mobley, T. A.; Petersen, T. H. *Acc. Chem. Res.* **1995**, *28*, 154.
- (22) Shilov, A. E.; Shul'pin, G. B. *Chem. Rev.* **1997**, *97*, 2879.
- (23) For a discussion on experiments using isotope effects to determine the intermediacy of alkane complexes in C–H activation see: Bullock, R. M. In *Transition Metal Hydrides*; Dedieu, A., Ed.; VCH: New York, 1992; pp 263–307.
- (24) Thompson, M. E.; Baxter, S. M.; Bulls, A. R.; Burger, B. J.; Nolan, M. C.; Santarsiero, B. D.; Schaefer, W. P.; Bercaw, J. E. *J. Am. Chem. Soc.* **1987**, *109*, 203.

complexes of coordinatively unsaturated electrophilic metal centers have also been used to explain stereochemical and rate data for olefin insertion reactions during polymerization of alkenes.^{26–31}

We previously reported that titanocene dimethyl is an efficient catalyst for the hydroboration of alkenes with catecholborane.³² This hydroboration was likely to proceed by a mechanism that is distinct from that of late transition metal hydroboration catalysts.^{33–38} Our initial investigations focused on the identification of the catalyst and revealed that the reaction of the titanocene dimethyl with catecholborane was the activating step since no reaction was observed between titanocene dimethyl and alkene at room temperature on the time scale of the catalytic process. These studies led to the discovery of a new class of σ -complex with unusual coordination of two catecholborane molecules to titanium through borane B–H bonds.^{39,40} The reaction chemistry of these novel bisborane complexes initiated fundamental studies of titanium borane complexes that contain this new type of metal–ligand interaction. We report here the synthesis of bisborane complex $\text{Cp}_2\text{Ti}(\text{HBcat}-4-t\text{-Bu})_2$ (**1a**) and its reactions with PMe_3 , PhSiH_3 , and PhCCPh that give complexes of the general formula $\text{Cp}_2\text{Ti}(\text{HBcat}-4-t\text{-Bu})(\text{L})$ where $\text{L} = \text{PMe}_3$, PhSiH_3 , and PhCCPh . This set of compounds raises questions concerning the borane bonding mode, factors controlling the stability of the compounds, and the mechanism of borane substitution that are also addressed in detail here.

Results

Synthesis of 1. A group of new titanocene σ -complexes with unusual coordination of neutral catecholborane through the B–H σ -bond was prepared (eq 1). The syntheses of these complexes are presented first. Because their spectroscopic data are not straightforward, spectral information will be presented in a separate section after the synthetic routes to the different compounds.



One member of this class of σ -complexes is $\text{Cp}_2\text{Ti}(\text{HBcat}')_2$ (**1a**), within which $\text{HBcat}' = \text{HBO}_2\text{C}_6\text{H}_3-4-t\text{-Bu}$. The reaction

(25) Zeigler, T.; Folga, E. *J. Am. Chem. Soc.* **1993**, *115*, 636.

(26) Brintzinger, H.; Beck, S.; Leclerc, M.; Stehling, U.; Roll, W. *Stud. Surf. Sci. Catal.* **1994**, *89*, 193.

(27) Clawson, L.; Soto, J.; Buchwald, S. L.; Steigerwald, M. L.; Grubbs, R. H. *J. Am. Chem. Soc.* **1985**, *107*, 3377.

(28) Cotter, W. D.; Bercaw, J. E. *J. Organomet. Chem.* **1991**, *417*, C1.

(29) Grubbs, R. H.; Coates, G. W. *Acc. Chem. Res.* **1996**, *29*, 85.

(30) Leclerc, M. K.; Brintzinger, H. H. *J. Am. Chem. Soc.* **1995**, *117*, 1651.

(31) Piers, W. E.; Bercaw, J. E. *J. Am. Chem. Soc.* **1990**, *112*, 9406.

(32) He, X.; Hartwig, J. F. *J. Am. Chem. Soc.* **1996**, *118*, 1696.

(33) Beletskaya, I.; Pelter, A. *Tetrahedron* **1997**, *53*, 4957.

(34) Dorigo, A. E.; Schleyer, P. v. R. *Angew. Chem., Int. Ed. Engl.* **1995**, *34*, 115.

(35) Westcott, S. A.; Blom, H. P.; Marder, T. B.; Baker, R. T. *J. Am. Chem. Soc.* **1992**, *114*, 8863.

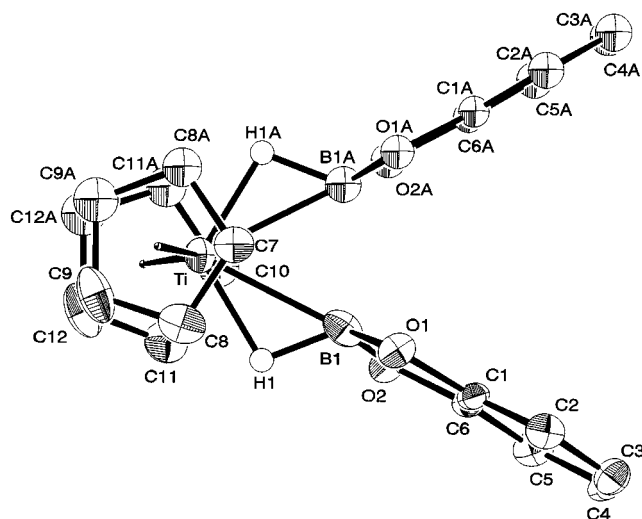


Figure 1. ORTEP of **1g**.

of titanocene dimethyl and 3 equiv of 4-*tert*-butylcatecholborane in pentane at -30°C for 8 h resulted in the precipitation of $\text{Cp}_2\text{Ti}(\text{HBcat}')_2$ (**1a**) as a yellow solid in 70% yield. Methane and *B*-methyl-4-*tert*-butylcatecholborane were also generated in this reaction as determined by ^1H NMR spectroscopy. At room temperature, compound **1a** is stable enough to be handled as a solid, but is unstable in solution. Complex **1a** was used as a precursor to new titanocene monoborane complexes as described in the next section. Five other analogues (**1b–f**) of complex **1a** were prepared in 11–83% yields by identical procedures using 3,5-di-*tert*-butylcatecholborane (**1b**), 4-methylcatecholborane (**1c**), 4-chlorocatecholborane (**1d**), 4-methylthiocatecholborane (**1e**), and 3-fluorocatecholborane (**1f**) instead of 4-*tert*-butylcatecholborane. The σ -complex containing unsubstituted catecholborane (**1g**) was also prepared. However, this analogue was insoluble in aromatic solvents after isolation. Thus, **1g** was characterized by solution NMR spectroscopy during its formation. Importantly, highly dilute reaction solutions deposited single crystals of **1g** that were suitable for X-ray diffraction, permitting structural characterization of these new compounds.

The connectivity of titanocene bisborane complexes was revealed by the X-ray crystallographic study of the parent bisborane complex **1g**. An ORTEP drawing is provided in Figure 1. Acquisition parameters for **1g** are provided in Table 1, and selected bond distances and angles are provided in Table 2. The Ti–B bond length was 2.335(5) Å. This distance is longer than the bond length in metallocene boryl complexes of tungsten (2.23 Å),⁴¹ tantalum (2.263 Å),⁴² and niobium (2.295 Å),⁴¹ despite the smaller size of titanium, and is indicative of a Ti–B bond order of less than 1. The B–Ti–B bond angle of 55° was too small for the complex to be a Ti(IV) bisboryl compound.⁴³ Indeed, the two hydrides were located in the difference map, and their presence was also determined by ^1H NMR spectroscopy.

(36) Evans, D. A.; Fu, G.; Anderson, B. A. *J. Am. Chem. Soc.* **1992**, *114*, 6679.

(37) Burgess, K.; van der Donk, W. A.; Westcott, S. A.; Marder, T. B.; Baker, R. T.; Calabrese, J. C. *J. Am. Chem. Soc.* **1992**, *114*, 9350.

(38) Burgess, K.; Ohlmeyer, M. J. *Chem. Rev.* **1991**, *91*, 1179.

(39) Hartwig, J. F.; Muhoro, C. N.; He, X.; Eisenstein, O.; Bosque, R.; Maseras, F. *J. Am. Chem. Soc.* **1996**, *118*, 10936.

(40) Muhoro, C. N.; Hartwig, J. F. *Angew. Chem., Int. Ed. Engl.* **1997**, *36*, 1510.

(41) Hartwig, J. F.; DeGala, S. R. *J. Am. Chem. Soc.* **1994**, *116*, 3661.

(42) Lantero, D. R.; Motry, D. H.; Ward, D. L.; Smith, M. R. *J. Am. Chem. Soc.* **1994**, *116*, 10811.

(43) Lauher, J. W.; Hoffmann, R. *J. Am. Chem. Soc.* **1976**, *98*, 1729.

Table 1. Acquisition Parameters for **1g**

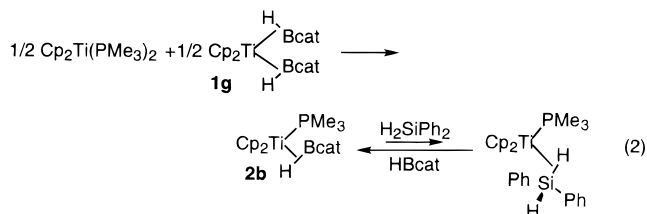
empirical formula	C ₂₉ H ₂₈ B ₂ O ₄ Ti	
formula weight	510.06	
color of crystal	pale yellow	
crystal system	monoclinic	
space group	P2 ₁ /m (no. 11)	
unit cell dimensions	a = 10.116(3) Å	β = 94.3710(10)°
	b = 10.077(2) Å	
	c = 12.222(1) Å	
Z value	2	
goodness of fit	1.92	
final R indices	R = 0.057	R _w = 0.064

copy (vide infra). The Ti–H distance was 1.74(4) Å, and the B–H bond length was 1.25(3) Å, typical of bridging titanocene hydrides.⁴⁴ These data are consistent with **1g** being a Ti(II) complex in which both hydrogen and boron have a bonding interaction with the metal center while preserving B–H bond character.

The most striking feature of this structure is the unusual geometry for a boron atom that has bonding interactions with four other atoms. The sum of the three angles at boron that do not include the hydride is 359.9°. This value indicates that the titanium, two oxygen atoms, and boron all lie in the same plane, that the catecholborane is drastically distorted, and that the boron is far from tetrahedral. Calculations of the geometry of Cp₂Ti[HB(OH)₂]₂ by density functional theory provided a similar unusual geometry.^{39,40} The hydrides of this model compound were located in a position similar to those identified in the Fourier difference map of **1g**, and the boron atom in the model compound also adopted a geometry in which the titanium, two oxygen atoms, and boron were coplanar.

Syntheses of 2–4: Ligand Substitution Reactions of 1. The reactivity of **1a** included diverse ligand substitution reactions as shown in Scheme 1. The catecholborane ligand in **1a** was displaced by CO, PMe₃, PhSiH₃, and PhCCPh to form titanocene dicarbonyl and new compounds **2–4**, respectively, as presented below. The reaction of compound **1a** at –30 °C with CO gave Cp₂Ti(CO)₂ in 88% yield and HBcat' in 93% yield. No intermediate corresponding to the product of substitution of one HBcat' ligand, Cp₂Ti(CO)(HBcat'), was observed. Further, there was no reaction between Cp₂Ti(CO)₂ and **1a** to form Cp₂Ti(CO)(HBcat').

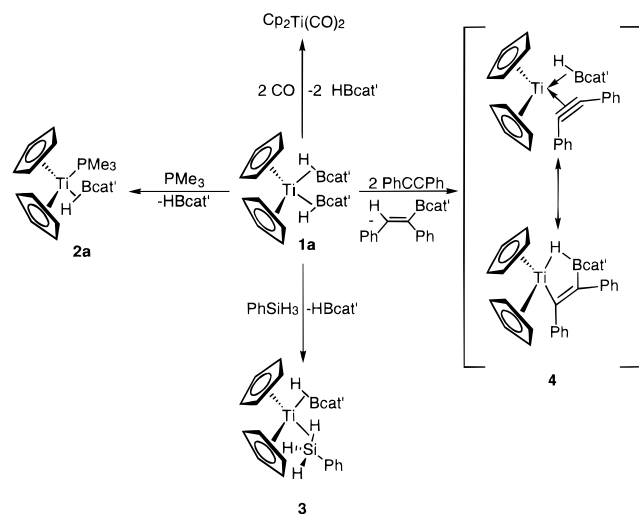
The reaction of compound **1a** with PMe₃ at –30 °C in toluene resulted in the formation of **2a** in 84% yield. However, attempts to isolate **2a** from this reaction mixture were unsuccessful. The product generated by this method was short-lived in the reaction medium at room temperature and decomposed to unidentified products. Attempts to isolate other analogues of **2a** from reaction mixtures of PMe₃ and corresponding complexes **1f,g** were also unsuccessful. Thus, the new route in eq 2 that generates no



reaction byproducts and involves an exact ligand stoichiometry was devised to allow for isolation of monoborane phosphine complexes. The reaction of compound **1g** and Cp₂Ti(PMe₃)₂ in

Table 2. Selected Bond Angles and Distances in **1g**

atom	atom	atom	angle (deg)	bond	distance (Å)
B1	Ti	B1A	53.8(2)	Ti–B	2.335(5)
H1	Ti	H1A	117(2)	Ti–H	1.74(4)
B1	Ti	H1	32(1)	B–H	1.25(3)
Ti	B1	H1	47(2)	B···B	2.11
Ti	H1	B1	101(2)	Cp1–Ti	2.44(1)
Ti	B1	O1	125.4(3)	Cp2–Ti	2.40(1)
Ti	B1	O2	126.0(3)		
O1	B1	O2	108.5(4)		
Cp1	Ti	Cp2	145.0(1)		

Scheme 1

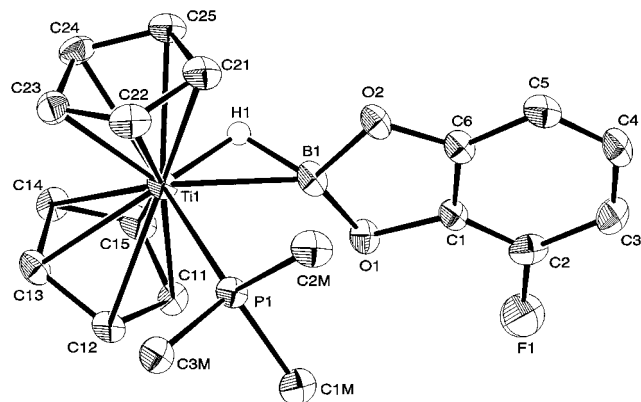
toluene at 0 °C generated a maroon solution containing Cp₂Ti(HBcat)(PMe₃) (**2b**). Cooling a solution of **2b** in toluene to –30 °C led to the precipitation of spectroscopically pure **2b** in 46% yield. Complex **2b** was unstable in solution at room temperature, but showed little degradation as a solid at room temperature over a few hours. The compound was stable as a solid for several weeks at –30 °C.

The phosphine borane complex **2b**, containing an unsubstituted catecholate substituent, was also generated by displacement of the coordinated silane in Cp₂Ti(H₂SiPh₂)(PMe₃)⁴⁴ by catecholborane (eq 2). Reaction of Cp₂Ti(H₂SiPh₂)(PMe₃) with 1 equiv of catecholborane in the presence of roughly 5 equiv of excess silane⁴⁵ formed **2b** in 56% yield while leaving 22% of Cp₂Ti(H₂SiPh₂)(PMe₃) unreacted. Reaction of **2b** with silane led to the formation of Cp₂Ti(H₂SiPh₂)(PMe₃) in 26% yield while leaving 55% of **2b** unreacted. These two experiments indicate that an equilibrium between the two complexes exists and that this equilibrium favors **2b** and free silane. Due to chemistry that competes with establishment of the equilibrium, we have not found conditions that allow for a quantitative analysis of this equilibrium.

The connectivity of compound **2a** was revealed by X-ray diffraction studies of the analogue Cp₂Ti(HBcat-3-F)(PMe₃) (**2c**) prepared from the 3-fluoro bisborane complex **1f** and Cp₂Ti(PMe₃)₂. An ORTEP diagram is provided in Figure 2. Acquisition parameters for **2c** are provided in Table 3, and selected bond distances and angles are provided in Table 4. The H–Ti–B bond angle of only 36° was too small to formulate **2c** as a Ti(IV) boryl hydride complex.⁴³ Further, the Ti–B bond length of 2.267(6) Å was, again, comparable to or longer than those in metallocene boryl complexes of W, Ta, and Nb, despite

(44) Spaltenstein, E.; Palma, P.; Kreutzer, K. A.; Willoughby, C. A.; Davis, W. M.; Buchwald, S. L. *J. Am. Chem. Soc.* **1994**, *116*, 10308.

(45) Because Cp₂Ti(H₂SiPh₂)(PMe₃) is unstable in the absence of added silane, excess silane was added to the sample before addition of borane.

Figure 2. ORTEP of **2c**.Table 3. Acquisition Parameters for **2c**

empirical formula	C ₁₉ H ₂₃ BFO ₂ PTi	
formula weight	392.05	
color of crystal	dark red	
crystal system	triclinic	
space group	P1	
unit cell dimensions	$a = 8.12190(10) \text{ \AA}$	$\alpha = 112.1880(10)^\circ$
	$b = 10.70550(10) \text{ \AA}$	$\beta = 94.3710(10)^\circ$
	$c = 11.66170(10) \text{ \AA}$	$\gamma = 98.4890(10)^\circ$
Z value	2	
goodness of fit	1.024	
final R indices	$R = 0.0638$	$R_w = 0.1631$

Table 4. Selected Bond Angles and Distances in **2c**

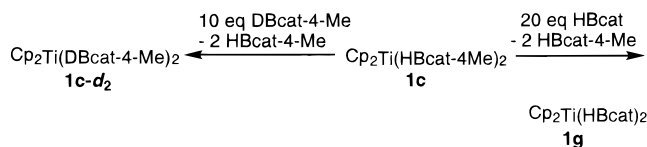
atom	atom	atom	angle (deg)	bond	distance (Å)
B1	Ti	H1	36(2)	Ti–B	2.267(6)
Ti	B1	H1	44(2)	Ti–H1	1.61(5)
H1	Ti	P	110(2)	B–H1	1.35(5)
B1	Ti	P	74.6(1)	Ti–P	2.522(2)
Ti	B1	O1	127.4(3)	Cp1–Ti	2.04(1)
Ti	B1	O2	126.1(4)	Cp2–Ti	2.05(1)
O1	B1	O2	106.2(4)		
Cp1	Ti	Cp2	136.2(1)		

the smaller size of Ti.^{41,42,46–52} The Ti–H bond distance of 1.61 Å is typical of bridging titanium hydrides.⁴⁴ These data again suggest the presence of a partial bond order among titanium, hydrogen, and boron in complex **2c**. Again the geometry at boron is remarkable and nearly identical to that in **1g**. The sum of the angles at boron that do not include the hydride is 359.7°. Thus, the boron again lies in the same plane as the titanium and two catecholate oxygens, and the geometry about this atom is far from tetrahedral.

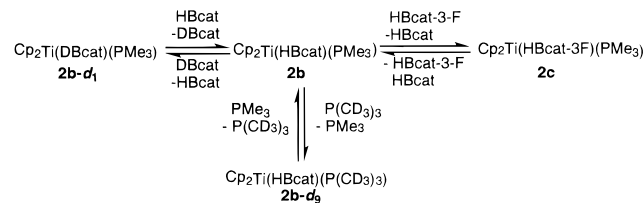
It is informative to make comparisons between the structure of this compound and that of Cp₂Ti(HBcat)₂ (**1g**). The Ti–B bond length in **2c** of 2.267(6) Å was shorter than that in **1g** (2.335(5) Å). The B–H bond length in **2c** (1.35(5) Å) was longer than that in **1g** (1.25(3) Å), while the Ti–H bond length in **2c** (1.61(5) Å) was shorter than the distance in **1g** (1.74(4) Å). While bearing in mind the ambiguity in hydride positions,

(46) Hartwig, J. F.; He, X. *Angew. Chem., Int. Ed. Engl.* **1996**, *35*, 315.(47) For example, the M–Cl bond length in Cp*₂Ti–Cl (2.363 Å) is shorter than the M–Cl distances in Cp*₂NbCl₂ and Cp*₂TaCl₂ of 2.439–2.483 Å.(48) Miao, F. M.; Prout, K. *Cryst. Struct. Commun.* **1982**, *11*, 269.(49) Prout, K.; Cameron, T. S.; Forder, R. A.; Critchley, S. R.; Denton, B.; Rees, G. V. *Acta Crystallogr., B* **1974**, *30*, 2290.(50) McCamley, A.; Miller, T. J. *Acta Crystallogr., C* **1994**, *50*, 33.(51) Labella, L.; Chernega, A.; Green, M. L. H. *J. Organomet. Chem.* **1995**, *C18*, 485.(52) Pattasina, J. W.; Heeres, H. J.; van Brouhuis, F.; Meetsma, A.; Teuben, J. H. *Organometallics* **1987**, *6*, 1004.

Scheme 2



Scheme 3



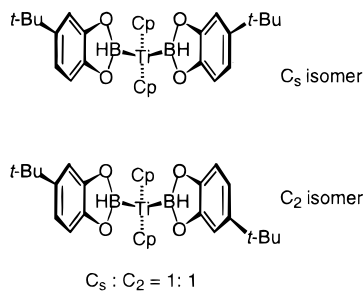
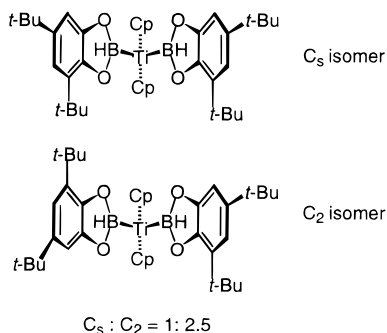
the trends in bond lengths may be attributed to differences in electron density at the titanium center in the two complexes. The basicity of the phosphine ligand would create a more electron-rich titanium center in complex **2c**. As a result, the structure of **2c** would lie further toward oxidative addition of catecholborane to Ti than does that of **1g**.

Reaction of **1a** with phenylsilane in toluene at -5°C for 5 h resulted in the formation of a yellow-green solution. Evaporation of toluene at -5°C , followed by washing of the resulting yellow solid with cold pentane, afforded Cp₂Ti(HBcat')(PhSiH₃) (**3**; HBcat' = HBO₂C₆H₃-4-*t*-Bu) in 65% yield as a spectroscopically pure material. Compound **3** is an unusual example of a complex ligated by two different types of X–H σ -bonds.

Complex **1a** reacted with 2 equiv of diphenylacetylene to form Cp₂Ti(PhCCPh)(HBcat') (**4**; HBcat' = HBO₂C₆H₃-4-*t*-Bu) and the vinyl boronate ester Ph(H)C=C(Ph)Bcat'. The alkyne complex **4** was unstable at -30°C and could not be isolated. As will be discussed in detail later, the vinyl boronate ester Ph(H)C=C(Ph)Bcat' and **1a** were formed by the decomposition of **4** if excess HBcat' was present. Cp₂Ti(PhCCPh) was the titanium product at these low temperatures if excess diphenylacetylene was present. Compound **4** was also prepared from the titanocene alkyne complex Cp₂Ti(PhCCPh). The reaction of 1 equiv of HBcat' with Cp₂Ti(PhCCPh) at -78°C for 10 min gave **4** in quantitative yield, as determined by ¹H NMR spectroscopy.

The bisborane σ -complexes were found to readily exchange borane ligand. For example, addition of catecholborane to a solution of **1c** in toluene-*d*₈ at -35°C generated free 4-methylcatecholborane and precipitated **1g** from solution (Scheme 2). Similarly, reaction between 10 equiv of DBcat-4-Me and **1c** at -10°C led to the observation of deuterium in the hydride position, as determined by ²H NMR spectroscopy of the reaction mixture. The monoborane phosphine complexes behaved analogously. For example, addition of 3-fluorocatecholborane to a solution of **2b** generated a mixture of **2b** and **2c** while addition of *B*-deuteriocatecholborane (DBcat) afforded a mixture of **2b** and **2b-d**₁ (Scheme 3). The phosphine ligand in **2b** was also readily exchanged. Trimethylphosphine-*d*₉ reacted with **2b** to generate a mixture of **2b** and its deuterated analogue **2b-d**₉.

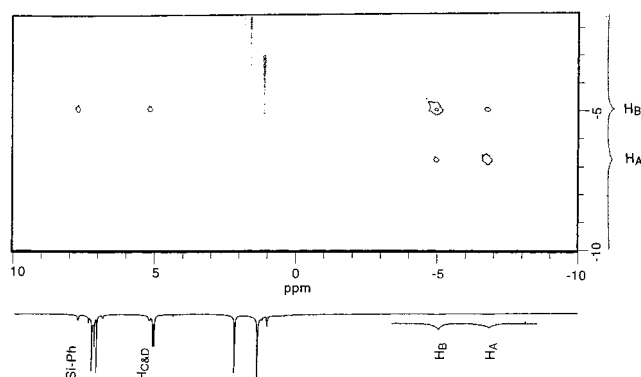
Spectroscopic Characterization. Compounds **1–4** were characterized by ¹H, ³¹P{¹H}, ¹¹B, and ¹H{¹¹B} NMR spectroscopy at -30°C . The bisborane complexes **1a–g** showed ¹¹B NMR signals between 45.7 and 46.3 ppm. The ¹H NMR spectra of these complexes contained characteristic broad hydride resonances between -5.37 and -5.85 ppm. The number and ratio of peaks in the Cp region varied depending on the number of substituents on the catechol aromatic ring. For

Figure 3. Isomers of complex **1a**.Figure 4. Isomers of complex **1b**.

example, the ^1H NMR spectrum of **1g**, containing no substituents on the catechol aromatic ring, displayed a single Cp resonance. However, the spectrum of **1a**, which contains a *tert*-butyl group at the 4-position in the aromatic ring of the catechol, revealed three Cp resonances in an approximate ratio of 1:1:2. These signals corresponded to equal ratios of the C_s (two Cp resonances) and C_2 (one Cp resonance) isomers of **1a** (Figure 3). These data indicated that **1a** exists as two isomers with different orientations of the *tert*-butyl groups of the catechol. Other analogues of **1a** with a single substituent on the catechol ring (**1c–f**) displayed a similar set of resonances in a 1:1:2 ratio in the Cp region, again due to equal amounts of the two isomers **1-C_s** and **1-C₂**. However, compound **1b**, which contains two bulky *tert*-butyl groups on the catechol ring, displayed a ^1H NMR spectrum containing three peaks in a ratio of 1:1:5, indicating that the ratio of the C_s isomer to the C_2 isomer was 1:2.5. The two hydride resonances in **1a** and **1c–f** were not resolved, but the hydride resonances for the two isomers of **1b** were resolved and were located at -5.37 and -6.15 ppm. We propose that the C_2 isomer of **1b** is the dominant isomer because the *tert*-butyl groups on the catecholate can be staggered (Figure 4). Infrared vibrations of the hydrides of **1a** were observed at 1722 and 1603 cm^{-1} , and the other bisborane derivatives showed bands between these values. Complex **1a-d₂** displayed no vibrations in this region but instead showed bands in the region between 1250 and 1160 cm^{-1} .

The NMR spectra of compounds **2a–c** were nearly identical, and *tert*-butyl-substituted compound **2a** is presented as an informative example. The ^{11}B NMR spectrum contained a single resonance at 64.0 ppm. The $^{31}\text{P}\{^1\text{H}\}$ NMR spectrum consisted of a sharp singlet at 29.3 ppm. The ^1H NMR spectrum displayed a broad signal at -9.7 ppm in addition to two doublets at 5.03 ppm ($J(\text{H,P}) = 2.70$ Hz) and 5.01 ppm ($J(\text{H,P}) = 2.40$ Hz) for the Cp ligands. The IR spectrum of **2b** contained a single broad band at 1650 cm^{-1} while the spectrum of **2b-d₁** displayed a band at an appropriate value of 1184 cm^{-1} .

Silane borane complex **3** displayed a signal at 37.1 ppm in the ^{11}B NMR spectrum. This signal lies significantly upfield of those for **1a–g** and **2a–c**. Signals for 4-coordinate boron are

Figure 5. Hydride region of the NOESY spectrum of **3**.

typically located upfield of those for 3-coordinate boron.⁵³ For example, the doublet in the ^{11}B NMR spectrum of free HBcat is shifted from δ 29 to δ 10.5 upon coordination by Et_3N to form the Lewis acid–base adduct $\text{HBcat}\cdot\text{Et}_3\text{N}$.^{39,54} Thus, the upfield shift in the ^{11}B NMR spectrum of **3** may indicate an increase in coordination number. The ^1H NMR spectrum of complex **3** displayed two hydride signals at δ -4.99 and -6.79 in addition to two Cp singlets at 4.99 and 4.95 ppm. The two uncoordinated silane hydrogens were observed as a single resonance at 5.00 ppm at -30°C , but were resolved into two resonances at 5.13 and 5.11 ppm at -80°C . A $^1\text{H}\{^{11}\text{B}\}$ NMR spectrum of **3** showed two sharp hydride signals. A NOESY spectrum of **3** was obtained with a mixing time of 300 ms at -80°C , at which the coordinated silane hydrogens do not undergo site exchange on the NMR time scale. The NOESY spectrum (Figure 5) showed NOE interactions with the titanium–borane hydride and the titanium-bound silane hydride, but not with the uncoordinated silane hydrogens. An NOE interaction was also observed between the titanium–silane hydride and the uncoordinated silane hydrogens. A ^2H NMR spectrum of $\text{Cp}_2\text{-Ti}(\text{DBcat})(\text{PhSiH}_3)$, synthesized using **1g-d₂** was obtained at -30°C . This spectrum revealed a resonance at 4.9 ppm corresponding to the chemical shift of the uncoordinated silane hydrogens, in addition to resonances at -4.98 and -6.78 ppm for the coordinated hydrides, indicating that exchange of the borane hydride with the silane hydrogens occurs on the laboratory time scale at -30°C . Complex **3** showed one sharp band at 2066 cm^{-1} in the IR spectrum for uncoordinated Si–H, along with broader bands between 1739 and 1840 cm^{-1} corresponding to the hydrides coordinated to titanium.

NMR spectroscopic characterization of alkyne complex **4** was conducted on a sample generated in situ by the addition of 1 equiv of HBcat' to a solution of $\text{Cp}_2\text{Ti}(\text{PhCCPh})$ in toluene- d_8 at -78°C . The ^{11}B NMR spectrum of **4** contained a resonance at 29.8 ppm, again upfield of those for **1a–g** and **2a–c**. The ^1H NMR spectrum of **4** contained a hydride signal at -1.59 ppm. This signal sharpened when decoupled from the boron nucleus, showing the presence of a B–H interaction. The deuterated analogue **4-d₁** was synthesized using DBcat' . Spectroscopic analysis of **4-d₁** by ^2H NMR revealed a single resonance at -1.59 ppm.

Mechanistic Studies of Ligand Substitution Reactions of 1a. Kinetic studies were conducted to investigate the mechanism of the reactions described above of compound **1a** with trimethylphosphine, carbon monoxide, phenylsilane, and dipheny-

(53) Nöth, H.; Wrackmeyer, B. *Nuclear Magnetic Resonance Spectroscopy of Boron Compounds*, 1st ed.; Springer-Verlag: New York, 1978; p 460.

(54) Goetze, R.; Nöth, H.; Pommerening, H.; Sedlak, D.; Wrackmeyer, B. *Chem. Ber.* **1981**, *114*, 1884.

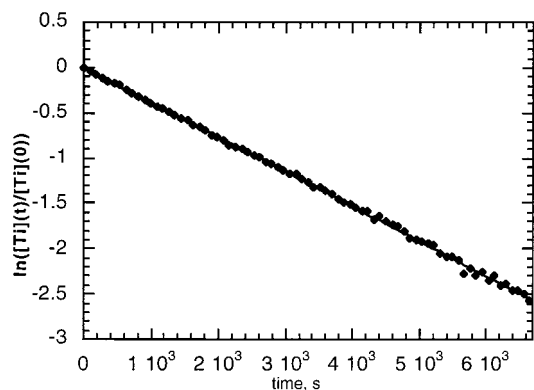


Figure 6. $\ln[[1a(t)]/[1a(0)]]$ vs time (s) for the reaction of PMe_3 with **1a**.

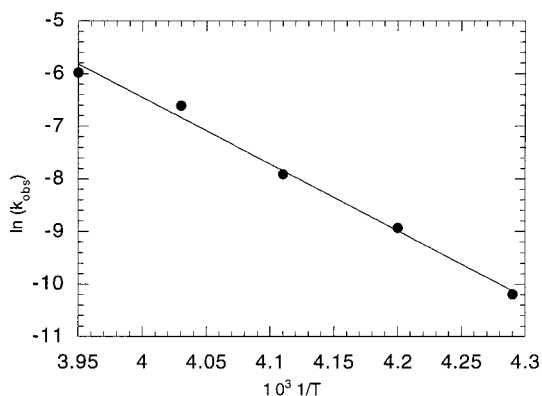


Figure 7. Eyring plot for the reaction of PMe_3 with **1a**.

Table 5. Values for the Observed Rate Constants at Various Concentrations of HBcat' and PMe_3 ^a

$[\text{PMe}_3]$, mmol	$[\text{HBcat}']$	k_{obs} ($\times 10^4, \text{s}^{-1}$)	$[\text{PMe}_3]$, mmol	$[\text{HBcat}']$	k_{obs} ($\times 10^4, \text{s}^{-1}$)
0.0568	0.0284	3.57	0.0473	0.0473	3.25
0.0568	0.0568	3.29	0.0785	0.0473	3.82
0.0568	0.0862	3.23	0.1421	0.0473	3.74

^aAll measurements were made at -30°C with $[1] = 0.00957 \text{ M}$.

lacetylene. With the exception of the studies on k_{obs} vs T , all kinetic studies were conducted using 9.6 mM solutions of **1a** in deuterated toluene at -30°C . The rates of the reactions were measured by monitoring the disappearance of the cyclopentadienyl ^1H NMR signal of **1a**.

Trimethylphosphine displaced one borane ligand in titanocene bisborane **1a** to form titanocene phosphine borane complex **2a**. The reaction rate was measured using HBcat' concentrations ranging from 0.0284 to 0.0852 M and PMe_3 concentrations ranging from 0.0474 to 0.142 M. The observed rate constants are shown in Table 5. The rate of this substitution reaction showed a first-order dependence on the concentration of bisborane complex as determined by a linear first-order plot (Figure 6). The rate constants for reactions containing no borane or 0.00284–0.0852 M added borane and the rate constants for solutions containing 0.0474–0.142 M added phosphine were $3.5 \times 10^{-4} \text{ s}^{-1}$ with a standard deviation of only $0.2 \times 10^{-4} \text{ s}^{-1}$. The constant values of k_{obs} with varied concentrations of HBcat' and PMe_3 demonstrated that the reaction was zero order in both borane and phosphine concentrations. Rate constants were measured over the temperature range of -15 to -40°C . The Eyring plot (Figure 7) provided the activation parameters $\Delta H^\ddagger = 24.7 \pm 2.8 \text{ kcal mol}^{-1}$, $\Delta S^\ddagger = 29.9 \pm 5.4 \text{ eu}$, and $\Delta G^\ddagger = 17.4 \pm 2.8 \text{ kcal mol}^{-1}$ at 233 K.

Table 6. Values of k_{obs} for Substitution Reactions by PMe_3 for Various σ -Complexes, $\text{Cp}_2\text{Ti}(\text{HBcat}')_2$

HBcat'	k_{obs} ($\times 10^4, \text{s}^{-1}$)
	1.31 ± 0.01
	3.5 ± 0.2
	6.5 ± 0.2
	2.15 ± 0.04
	2.75 ± 0.09

To test potential bonding models and transition state structures for displacement reactions, we determined the effect of the borane steric and electronic properties on the rate of substitution by phosphine. To this end, a series of titanocene borane σ -complexes were synthesized using different catecholboranes. The rate constants for the substitution of the boranes by PMe_3 were measured for each of **1a–e** and are presented in Table 6. In general, more electron-withdrawing substituents on the aromatic ring of the catecholborane ligand decreased the rate of substitution. For example, the electron-poor 4-chloro complex **1d** underwent substitution 3 times slower than electron-rich 4-methyl complex **1c**.⁵⁵ The 4-methylthio complex **1e**, which is slightly more electron-rich than complex **1d** but less electron-rich than **1c**, underwent substitution slightly faster than did **1d** and about 2 times slower than did **1c**. Surprisingly, the rate of the reaction *decreased* with increased steric bulk of the borane ligands. Di-*tert*-butyl compound **1b** underwent ligand substitution at the slowest rate. Complex **1a** with only one *tert*-butyl ligand on the catechol ring reacted 3 times faster than did **1b**, while 4-methyl complex **1c** reacted 5 times faster than did **1b**.

Carbon monoxide displaced both of the borane ligands in complex **1a** to form $\text{Cp}_2\text{Ti}(\text{CO})_2$. The rate of this reaction was $(3.7 \pm 0.6) \times 10^{-4} \text{ s}^{-1}$. The reaction rate was measured using concentrations of added HBcat' of 0.0474–0.237 M and CO pressures of 0.5–3.0 atm. The reaction of **1a** with CO displayed a first-order dependence on **1a** and a zero-order dependence on both borane and CO. This absence of reaction order in the incoming or departing ligand is identical to that observed for the reaction of **1a** with PMe_3 .

The rate constant for the reaction of **1a** with PhSiH_3 to form silane–borane complex **3** was $(4.2 \pm 0.1) \times 10^{-4} \text{ s}^{-1}$. The reaction showed a first-order rate dependence on the concentration of **1a**. Linear first-order plots were observed with no added HBcat' and with only 1 equiv of added silane, suggesting that the reaction was again zero order in both departing and incoming ligands. The k_{obs} value similar to those of the reaction of **1a** with PMe_3 and CO and the absence of an order in HBcat' and

(55) The electronic properties of the borane can be systematically perturbed by changing the identity of the substituent on the aromatic ring of the catecholborane. Hammett substituent constants for the respective benzoic acids were used to estimate the electronic properties of the boranes, bearing in mind that the substituents have different σ parameters when located in the metal and para positions. The electrophilicity of the boranes should decrease in the trend $\text{HBcat-4-Cl} > \text{HBcat-4-SMe} > \text{HBcat} > \text{HBcat-4-Me}$. Connors, K. A. *Chemical Kinetics: the study of reaction rates in solution*, 1st ed.; VCH: New York, 1990; p 480.

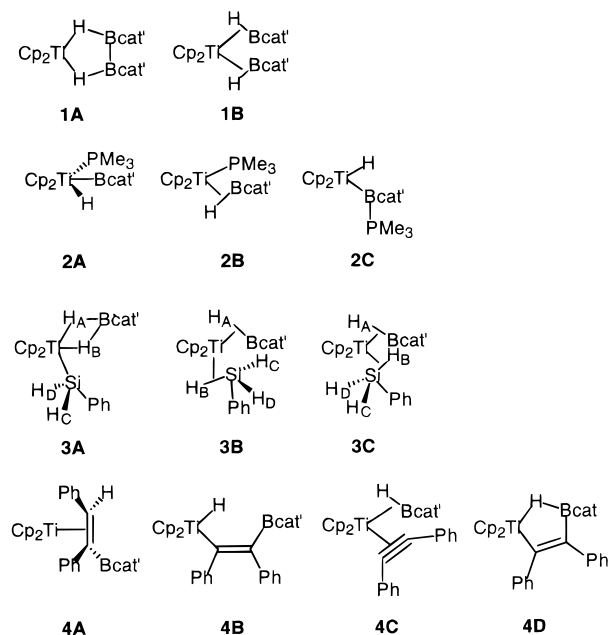


Figure 8. Possible structures for complexes 1–4.

PhSiH₃ indicate that the reaction proceeded by a similar mechanism.

The reaction of **1a** with diphenylacetylene formed the alkyne addition product **4**. This reaction showed a first-order rate dependence on the concentration of **1a**. The reaction rate was measured at concentrations of PhCCPh from 0.0474 to 0.237 M and concentrations of HBcat' from 0.0189 to 0.0474 M. The observed rate constant for these reactions was $(3.8 \pm 0.1) \times 10^{-4} \text{ s}^{-1}$. The consistency of the k_{obs} values at varied concentrations of PhCCPh and HBcat' showed that the reaction was zero order in HBcat' and PhCCPh.

Complex **4** was unstable in solution at -30°C and formed the alkyne complex $\text{Cp}_2\text{Ti}(\text{PhCCPh})$ in the presence of diphenylacetylene. In this reaction the diphenylacetylene in **4** was hydroborated and eliminated as the vinyl boronate ester $\text{Ph}(\text{H})\text{C}=\text{C}(\text{Ph})\text{Bcat}'$. The observed rate constant for this hydroboration reaction was $(5.5 \pm 0.3) \times 10^{-4} \text{ s}^{-1}$.

We investigated the steric effects of the borane ligands on the rates of this hydroboration process. The alkyne–borane complexes $\text{Cp}_2\text{Ti}(\text{PhCCPh})(\text{Bcat}-4\text{-Me})$ and $\text{Cp}_2\text{Ti}(\text{PhCCPh})(\text{Bcat}-3,5\text{-di-}t\text{-Bu})$ were synthesized by reacting $\text{Cp}_2\text{Ti}(\text{PhCCPh})$ with 4-methylcatecholborane and 3,5-di-*tert*-butylcatecholborane, respectively. The observed rate constants for the formation of vinyl boronate esters from these complexes were $(2.83 \pm 0.03) \times 10^{-4} \text{ s}^{-1}$ for formation of $\text{Ph}(\text{H})\text{C}=\text{C}(\text{Ph})\text{Bcat}-4\text{-Me}$ and $(16.8 \pm 0.2) \times 10^{-4} \text{ s}^{-1}$ for formation of $\text{Ph}(\text{H})\text{C}=\text{C}(\text{Ph})\text{Bcat}-3,5\text{-di-}t\text{-Bu}$. Our results indicate that vinyl boronate ester formation occurred faster from complexes containing more sterically demanding boranes.

Discussion

Spectroscopic and Structural Studies. An understanding of the structures of the novel coordination complexes **1–4** was one focus of our study. Spectroscopic studies indicated that each complex exhibited some degree of partial bonding and that the overall structural description is most accurately depicted as a resonance hybrid. NMR properties of the complexes were employed to determine the limiting structures that most closely resembled the observed structure. Possible structures of complexes **1–4** are presented in Figure 8, and the rationale for

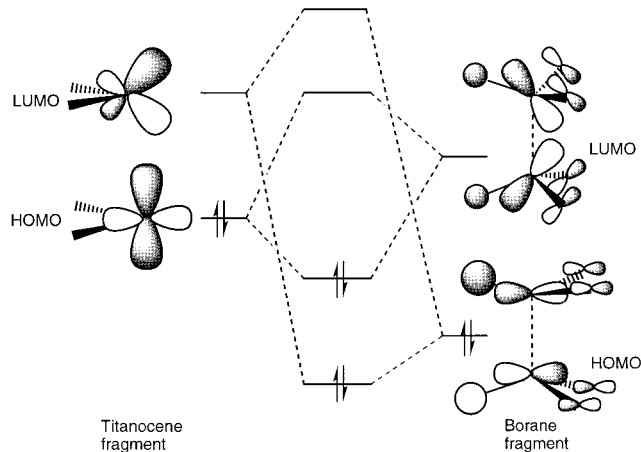


Figure 9. The two dominant orbital interactions in bisborane σ -complexes reveal that the titanocene fragment and the boranes have correct symmetry for overlap. Importantly, the borane LUMO possesses significant p-orbital character.

selection of the limiting structure that most closely resembles each of the observed species will be presented in this section.

The observed ^{11}B NMR shifts of **1a–g** located between 45 and 46 ppm are downfield of free catecholborane, indicating an interaction of the boron with the titanium metal center.^{41,42,56} The ^1H NMR spectra of **1a** displayed a broad hydride signal at -5.7 ppm, which sharpened upon decoupling from boron. The upfield shift of this signal was indicative of a d^2 metal center, and the sharpened $\{^{11}\text{B}\}^1\text{H}$ NMR signal suggested a B–H interaction. The IR bands of **1a–g** between 1599 and 1722 cm^{-1} were reduced from that for catecholborane ($\nu = 2660 \text{ cm}^{-1}$), indicating a reduction in B–H bond order, as are $\nu_{\text{X-H}}$ values in agostic and σ -complexes. All these data suggest that **1B** is the structural extreme most closely resembling the observed complex **1a**.

In collaborative work, we had previously reported extended Hückel calculations on $\text{Cp}_2\text{Ti}(\text{HB}(\text{OH})_2)_2$, a model for compound **1a**. These studies indicated that there is some electron density between the two boron atoms. However, the B–B distance of 2.11 \AA , which is $0.23\text{--}0.25 \text{ \AA}$ longer than those in polynuclear $\text{B}_2\text{H}_6^{2-}$ complexes,^{57,58} suggests that interaction between the two boron atoms is small.

In addition, these calculations provided a description of the bonding interactions in the borane complexes (Figure 9). As one might expect from other σ -complexes, these studies indicated that the LUMO of the titanocene fragment and the HOMO of the borane, which contains the antisymmetric combination of the B–H σ -bonding orbitals, have the proper symmetry for overlap.³⁹ Further, this interaction involving donation of electron density from the X–H σ -bond is supplemented by back-donation from the metal HOMO into the ligand LUMO, as it is for most σ -complexes. However, the ligand LUMO in this case is a boron p-orbital rather than a σ^* -orbital as it is in other dihydrogen, silane, or alkane complexes. This distinction is important because the boron p-orbital is lower in energy than a σ^* -orbital, creating a closer energy match with the metal d-orbitals and a stronger σ -complex than many previous alkane, dihydrogen, or silane complexes. Further, this back-bonding can be used to rationalize the unusual geometry at boron we observed by X-ray diffraction. Maximum overlap

(56) Hartwig, J. F.; Huber, S. *J. Am. Chem. Soc.* **1993**, *115*, 4908.

(57) Kaez, H. D.; Fellmann, W.; Wilkes, G. R.; Dahl, L. F. *J. Am. Chem. Soc.* **1965**, *87*, 2755.

(58) Andersen, E. L.; Felhner, T. P. *J. Am. Chem. Soc.* **1978**, *100*, 4606.

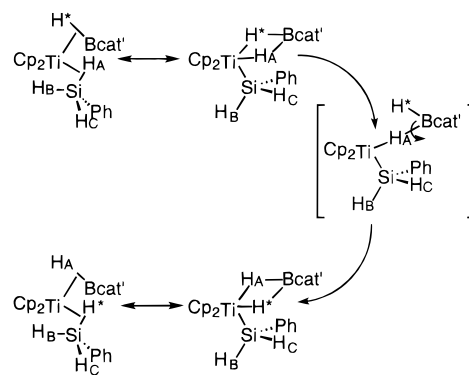
of the metal HOMO with the borane LUMO will exist when the titanium, boron, and catecholate oxygens are coplanar.

The phosphine monoborane complexes **2a–c** could be described by the two structural extremes **2A** and **2B** in Figure 8 or the isomeric **2c**. The ambiguity of the hydride positions in the X-ray crystallographic study makes spectroscopic studies more capable than X-ray crystallography of distinguishing **2a** from **2b**. The ^{11}B NMR spectra of compounds **2a–c** all showed a signal near 64 ppm located downfield of free catecholborane and consistent with both structures **2A** and **2B**. Further, the sharp signals in the ^{31}P NMR spectra of **2a–c** and the doublet cyclopentadienyl resonance for **2a** that collapsed to a singlet upon decoupling from phosphorus showed that the phosphine was bound to the metal center and not the quadrupolar boron nucleus. The ^1H NMR spectra of **2a–c** also contained a broad resonance between -9.4 and -9.8 ppm, which sharpened upon decoupling from boron. The downfield shift contrasts the sharp upfield signal that would be expected for a Ti(IV) hydrido boryl complex because related complexes show sharp hydride signals.^{41,42} These data reveal the presence of a B–H interaction in compounds **2a–c** and indicate that the metal center is best described as a Ti(II) d^2 center and not a Ti(IV) d^0 center. The broad band at 1650 cm^{-1} in the IR spectrum of **2b** indicated a weakened B–H bond, but the small B–Ti–H angle and the short B–H distance support a partial B–H bonding interaction. Thus, limiting structure **2B** most closely resembles complexes **2a–c**.

Complex **3** is the product from the substitution of one borane ligand in **1a** by PhSiH_3 . A structure for **3** in which the hydrides occupy the endo positions and the boryl and silyl groups occupy the exo positions is unreasonable because this structure would maximize steric interaction between the ligand aryl groups and the Cp ligands. Three possible structures for compound **3**, in which unfavorable interaction is minimized, are presented in Figure 8, and spectroscopic methods were again used to distinguish between them. The ^{11}B NMR spectrum of **3** contained a signal at 37 ppm, while the ^1H NMR spectrum revealed two broad signals at -4.98 and -6.78 ppm. Structure **3A**, in which boron is 4-coordinate and anionic, can be ruled out as the dominant resonance contributor by the ^{11}B NMR chemical shift that is downfield of free HBcat' . Two-dimensional ^1H NMR spectroscopy was used to differentiate between structures **3B** and **3C**. NOE interactions were observed between the bridging borane hydride (H_A) and the bridging silane hydride (H_B) and between the silane uncoordinated hydrogens (H_C , H_D) and H_B . No interactions were observed between H_A and either H_C or H_D . These data indicate that **3** exists as the regioisomer **3C** and that potential residual turnstile rotation of the silane does complicate the interpretation of the NOE experiment. Two sharp infrared bands ($\nu = 2051$ and 2095 cm^{-1}), which were attributed to the vibrations of the uncoordinated silane hydrogens, H_C/H_D , along with broad bands between 1754 and 1863 cm^{-1} corresponding to the silane and borane hydrides also supported structure **3C**. The 1754 and 1863 cm^{-1} values are close to those of other titanium–silane complexes that possess weakened X–H bonds.⁴⁴ Although structure **3C** appears to be the dominant resonance form of compound **3**, the ^{11}B NMR chemical shift that is upfield of that for compounds **1a–g** and **2a–c** implies that there is a significant contribution from **3A** to the overall structure.

The site exchange of the hydrogen atoms in **3** was revealed by ^2H NMR spectroscopy and corroborates the substantial borohydride character in **3**. Metallocene borohydride complexes are known to undergo hydrogen exchange processes with low

Scheme 4



activation barriers ($5\text{--}10\text{ kcal mol}^{-1}$).⁵⁹ Thus, the deuterium label may scramble from the borane to the silane through a bidentate–monodentate equilibrium (Scheme 4) in which rotation of the monodentate borohydride would cause the label to be exchanged into the silane. Once incorporated into the silane hydride position, the deuterium label may exchange with the uncoordinated silane hydrogen positions by a turnstile rotation similar to that in agostic complexes.⁶⁰

The structure of alkyne adduct **4** was deduced by NMR spectroscopy. Four possible structures for **4** are presented in Figure 8. The ^{11}B NMR spectrum of **4** consisted of a resonance at 29.4 ppm, while the ^1H NMR spectrum contained a broad hydride peak at -1.59 ppm. This hydride signal sharpened when decoupled from boron, indicating a bonding interaction between boron and hydrogen. On the basis of these data, **4A** and **4B**, which would show hydride resonances in the vinyl region of η^2 -coordinated vinyl boronate esters⁶¹ and in the region of Ti(IV) hydrides,^{62,63} respectively, can be eliminated as possible structures of **4**. The ^{11}B NMR resonance of 29.4 ppm, which is nearly equivalent to that of catecholborane, and the broad hydride signal at $\delta -1.59$, which is slightly downfield of the resonances of other borane complexes (**1–3**) and upfield of the resonances of d^0 metallocene borohydrides,⁶⁴ suggest that the structure of **4** results from nearly equivalent contributions from a σ -bonded borane compound (**4C**) and an η^2 -vinyl hydride complex (**4D**).⁶¹ This conclusion is consistent with the reactivity of **4**. Rapid exchange of the borane ligand with free borane would be expected from a complex with structure **4C**, while spontaneous elimination of $\text{H}(\text{Ph})\text{C}=\text{C}(\text{Ph})(\text{Bcat}')$ would be expected from a complex such as **4D**. Both processes were observed.

Mechanistic Studies. Kinetic studies were conducted to investigate the mechanism of ligand substitution by PMe_3 . The mechanisms of these reactions were investigated for two principal reasons. First, the mechanism of the substitution reactions would probe whether the B–H bond of the borane was acting as a simple two-electron, dative ligand. If **1a–e** contained an anionic $\text{H}_2\text{B}_2\text{cat}'_2$ ligand rather than two neutral borane ligands, simple borane displacement would be unlikely to occur. Second, if the mechanism of substitution were dissociative, then we could obtain experimental values for the enthalpy of activation. In general, the enthalpies of activation

(59) Marks, T. J.; Kolb, J. R. *Chem. Rev.* **1977**, *77*, 263.

(60) Brookhart, M.; Green, M. L. H. *J. Organomet. Chem.* **1983**, *250*, 395.

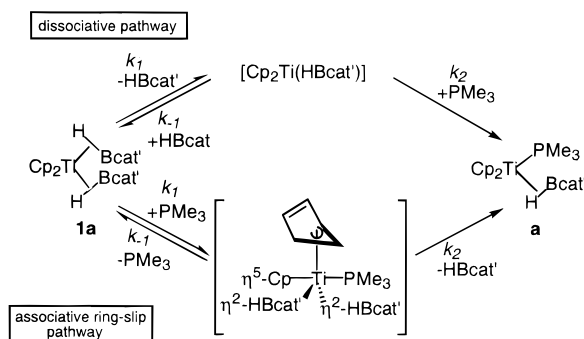
(61) Binger, P.; Sandmeyer, F.; Krüger, C.; Kühnigk, J.; Goddard, R.; Erker, G. *Angew. Chem., Int. Ed. Engl.* **1994**, *33*, 197.

(62) Bercaw, J. E.; Brintzinger, H. H. *J. Am. Chem. Soc.* **1972**, *94*, 1219.

(63) Bennet, J. L.; Wolczanski, P. T. *J. Am. Chem. Soc.* **1994**, *116*, 2179.

(64) Davies, N.; James, B. D.; Wallbridge, M. G. H. *J. Chem. Soc. A* **1969**, 2601.

Scheme 5



in dissociative ligand substitution reactions are similar to the bond dissociation energies of the ligand–metal bond. From the values of ΔH^\ddagger , we could provide an upper limit on the strength of the Ti–(HBcat) σ -bond. Two possible pathways for ligand substitution in **1a** are presented in Scheme 5. The associative pathway depicts a mechanism involving an η^5 – η^3 ring slip of the Cp ligands followed by addition of a ligand. The second pathway involves dissociation of a ligand to form a coordinatively unsaturated intermediate, which is rapidly trapped by the incoming ligand.

Associative ligand substitution reactions of coordinatively saturated metallocenes commonly proceed via ring slip mechanisms.^{65,66} Such mechanisms occur less frequently in first-row transition metal complexes where the small sizes of the metal centers disfavor associative processes, and weak metal–ligand bonds favor dissociative processes. An initial ring slip followed by coordination of PMe_3 would result in the formation of an η^3 -cyclopentadienyl complex. This complex could then undergo borane dissociation and resume the η^5 -cyclopentadienyl coordination mode to generate **2a**. The rate of the reaction by this mechanism may be expressed as in eqs 3 and 4. The rate of a reaction by this pathway would be first order in **1a** and PMe_3 and zero order in borane.

$$\text{rate} = \frac{k_1 k_2 [\mathbf{1a}] [\text{PMe}_3]}{k_{-1} + k_2} \quad (3)$$

$$\text{rate} = k_{\text{obs}} [\mathbf{1a}] [\text{PMe}_3] \quad (4)$$

$$\text{where } k_{\text{obs}} = \frac{k_1 k_2}{k_{-1} + k_2}$$

$$\text{rate} = \frac{k_1 k_2 [\mathbf{1a}] [\text{PMe}_3]}{k_{-1} [\text{HBcat}'] + k_2 [\text{PMe}_3]} \quad (5)$$

Dissociative mechanisms are common for ligand substitution in coordinatively saturated first-row transition metal complexes. In such a mechanism, initial dissociation of one borane ligand from **1a** would occur to generate a monoborane intermediate, which would be rapidly trapped by PMe_3 to form **2a** (Scheme 5). The rate expression for this mechanism is shown in eq 5. If the rate of phosphine coordination is much faster than the rate of borane recoordination, then the overall reaction rate would have a concentration dependence on only **1a**. However, if the rate of phosphine coordination is much slower than the rate of borane recoordination, then the rate of the overall reaction would have a first-order dependence on the concentrations of **1a** and PMe_3 and would have an inverse first-order dependence on the concentration of HBcat'.

(65) Palmer, G. T.; Basolo, F.; Kool, L. B.; Rausch, M. D. *J. Am. Chem. Soc.* **1986**, *108*, 4417.

(66) For an early example with monocyclopentadienyl compounds see: Schuster-Woldan, H. G.; Basolo, F. *J. Am. Chem. Soc.* **1966**, *88*, 1657.

Our kinetic studies indicated that the ligand substitution reaction has a first-order dependence on the concentration of **1a** and no dependence on the concentration of either borane or PMe_3 . These data are inconsistent with the conventional ring slip pathway.⁶⁷ Instead, these data support the mechanism involving initial dissociation of the catecholborane ligand, followed by rapid association of PMe_3 to form **2a**. Thus, $k_2 \gg k_{-1}$ in eq 5, and HBcat' dissociation is irreversible and rate determining in these reactions.

The reaction rates of dissociative ligand substitutions with initial irreversible ligand dissociation are independent of the nature of the incoming ligand. Our results are consistent with this requirement. Complex **1a** reacted with trimethylphosphine, carbon monoxide, phenylsilane, and diphenylacetylene with equal rate constants. These data confirm our conclusions based on the dependence of rate on the concentrations of HBcat' and PMe_3 .

Finally, a ΔS^\ddagger value that is positive is commonly observed for dissociative substitution because of the lengthening of the M–L bond during formation of the transition state, and accompanying increase in the degrees of freedom.⁶⁸ The entropy of activation for the reaction of **1a** with PMe_3 was 30 ± 5 eu, consistent with a dissociative mechanism. The ΔH^\ddagger value of 25 ± 3 kcal mol⁻¹ provided an upper limit for the Ti–(B–H) bond dissociation energy which was intermediate in strength between those of known silane (~ 30 kcal mol⁻¹) and dihydrogen (~ 13 kcal mol⁻¹) σ -complexes of other metal systems.^{2,3} The similar energy of borane and silane σ -complexes is consistent with our observation of an equilibrium between phosphine borane complex **2a** and $\text{Cp}_2\text{Ti}(\text{H}_2\text{SiPh}_2)(\text{PMe}_3)$.

Kinetic studies were conducted on a series of titanocene borane σ -complexes to investigate the effect of the steric and electronic properties of the borane ligand on the substitution reaction. This study was performed by measuring the rate constants of substitution for different σ -complexes synthesized from boranes with different substituents on the catecholate ring (Table 6). Because the mechanism was dissociative, a trend in the strength of the Ti–(HBcat) interaction as a function of electronic factors could be established from rate constants. The observed trend is more likely to result from changes in the strength of the Ti–(HBcat) interaction than perturbations of the free H–B bond strength since BDEs of boranes change only slightly with variation of substituents.⁶⁹ It should be noted that the metal–borane BDEs may be different from enthalpies of activation because of the significant reorganization detected by the anomalous steric effects. This phenomenon, however, does not preclude comparisons of activation parameters as long as the steric factors are relatively constant. Thus, we conducted our studies on electronic effects using substituents of similar size.

Our results indicated that complexes with electron-withdrawing substituents on the aromatic ring of the catecholborane underwent substitution reactions more slowly than did those with more electron-donating substituents. This observation suggests that σ -borane complexes are stabilized by increasing the degree of electron back-donation from titanium. This result is consistent with the importance of back-bonding between the titanium HOMO and the borane LUMO used above to rationalize the

(67) A less conventional ring slip mechanism involving an intramolecular and irreversible rate-determining transformation from an η^5 to an η^3 cyclopentadienyl complex is less consistent with the large positive entropy of activation and steric effects described below.

(68) Atwood, J. D. *Inorganic and Organometallic Reaction Mechanisms*; Cole Publishing Co.: Monterey, CA, 1985; p 17.

(69) Rablen, P. R.; Hartwig, J. F.; Nolan, S. P. *J. Am. Chem. Soc.* **1994**, *116*, 4121.

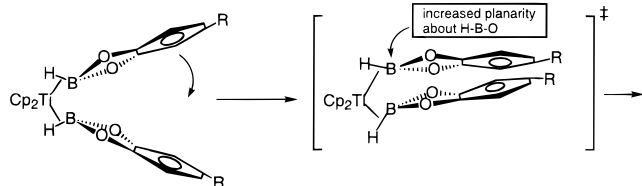


Figure 10. Proposed mechanism for structural rearrangement of catecholborane ligands prior to dissociation.

stability and geometry of the borane σ -complexes. A more electrophilic borane would create a greater back-bonding interaction and a stronger overall metal–borane bonding interaction. In addition, the greater stability we observed of the phosphine–borane complex **2a**, relative to that of $\text{Cp}_2\text{Ti}(\text{H}_2\text{-SiPh}_2)(\text{PMe}_3)$, is likely to result from the same back-bonding interaction. The metal will interact more strongly with the borane LUMO.

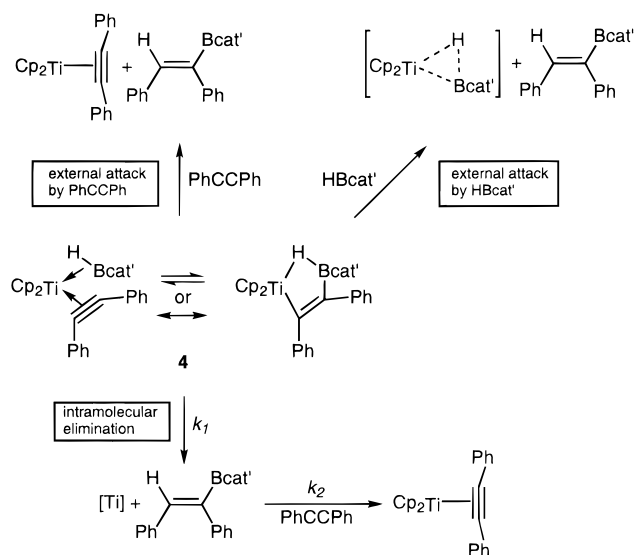
The steric effects on the substitution reactions were unusual. Classic dissociative ligand substitution reactions typically proceed faster with larger departing ligands. Contrary to this usual trend, we found that increasing steric bulk on the catechol resulted in a *decrease* in the rate of substitution by PMe_3 . These observations are more common for an associative mechanism. However, the reproducibility of numerous kinetic experiments, the independence of the reaction rate on the nature of the incoming ligand, and the values of the activation parameters clearly show that the mechanism for the borane substitution reactions is dissociative.

The unusual steric effects can be explained by the structural changes in Figure 10. The free catecholborane product is planar. Thus, the departing borane will be flatter in the transition state than it is in the ground state. The flattening of the catecholborane requires that its aromatic ring swing toward that of the nondissociating borane. The initial titanium product is $[\text{Cp}_2\text{Ti}(\text{HBcat}-4\text{-R})]$ which could be formulated as either a Ti(IV) hydrido boryl or Ti(II) monoborane σ -complex. The geometry of this intermediate is not simple to predict. To form a boryl hydride complex, the boryl or hydride group would presumably relocate to the side of the titanocene wedge formerly occupied by the dissociating ligand. However, in a monoborane complex intermediate, the location of the borane ligand may be relatively unchanged because Cp_2ML complexes that are low spin d^2 are predicted to be nonsymmetric.⁴⁵ Thus, it is not clear whether rearrangements of the remaining borane would exacerbate the steric effects of the flattening of the departing borane. However, the transition state is likely to have greater steric interactions in either case than would the ground state because of the geometrical changes of the departing borane. Complexes with more structurally hindered boranes would undergo dissociation more slowly.

Diphenylacetylene reacted with **1a** to form the alkyne complex **4**. The rate of this substitution reaction was the same as those for borane substitution by other incoming ligands. However, the product **4** was unstable in solution at -30°C . Compound **4** reacted further with diphenylacetylene to generate $\text{Cp}_2\text{Ti}(\text{PhCCPh})$ and vinyl boronate ester. This transformation of **4** to $\text{Cp}_2\text{Ti}(\text{PhCCPh})$ and vinyl boronate ester is related to the mechanism of catalytic hydroboration of alkynes by Ti(II) complexes.³² To study the reaction of **4** with diphenylacetylene, the alkyne complex **4** was independently prepared by the reaction of $\text{Cp}_2\text{Ti}(\text{PhCCPh})$ with catecholborane.

Three potential mechanisms for the hydroboration reaction are shown in Scheme 6. One possible mechanism may involve external attack by diphenylacetylene on coordinated HBcat' . The

Scheme 6



borane ligand in the alkyne–borane complex **4** presumably has a significantly weakened B–H bond. This property may activate the borane ligand in **4** toward addition across an uncoordinated alkyne. In this case, the ligated diphenylacetylene would remain on the metal to form the metal–alkyne product. This mechanism would provide a first-order rate dependence on the concentrations of both diphenylacetylene and **4** and a zero-order dependence on the concentrations of borane.

In an alternative mechanism, the ligated alkyne in **4** could undergo electrophilic attack by external HBcat' , particularly in reactions containing excess borane. This reaction would release the vinyl boronate ester product and generate the Ti(IV) hydrido boryl or Ti(II) monoborane complex. The fate of this intermediate would depend on the reagents in solution. In the presence of borane, **1a** would be generated; in the presence of alkyne, **4** would be generated. In either case, this pathway would show a first-order rate dependence on the concentration of borane and **4**, and a zero-order dependence on alkyne.

Finally, it might be expected from the proposed structure of **4** that reductive elimination of vinyl boronate ester would be facile. A simple reductive elimination involving the hydride and the Ti–C bond would form the vinyl boronate ester and release the Cp_2Ti fragment, which would rapidly react with alkyne to form $\text{Cp}_2\text{Ti}(\text{PhCCPh})$. This mechanism would provide a zero-order dependence of the reaction rate on both borane and alkyne concentration and a simple first-order dependence on the concentration of **4**.

Our kinetic studies indicated that the formation of vinyl boronate ester from **4** proceeded with a first-order dependence on the concentration of **4** and a zero-order dependence on the concentrations of both borane and alkyne. These results eliminated initial external attack by either borane or alkyne onto **4** as possible mechanisms for the reaction. Therefore, the most plausible mechanism for the hydroboration of alkyne in **4** is, indeed, the intramolecular reductive elimination.

It should be noted, however, that a zero-order dependence on HBcat' and alkyne could also result from a combination of borane dissociation followed by external attack by HBcat' on the unsaturated intermediate (Scheme 7). Borane dissociation from **4** is reasonable because **4'** is a resonance contributor to the overall structure of the alkyne borane complex. However, dissociation of borane and reaction of free borane with $\text{Cp}_2\text{Ti}(\text{PhCCPh})$ by addition of the B–H bond across the Ti–C bond

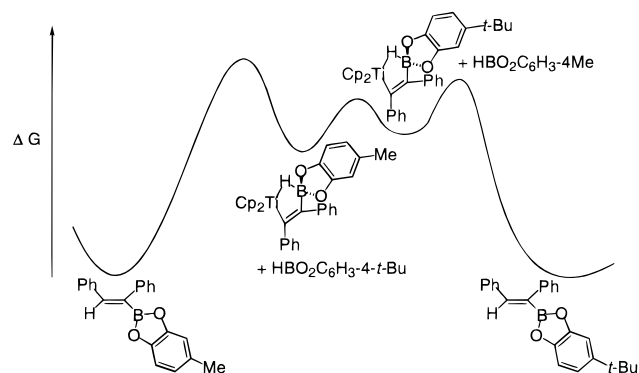
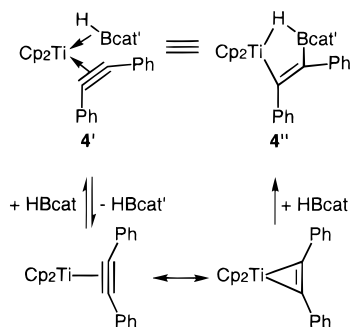


Figure 11. Qualitative free energy diagram for borane exchanges in **4**.

Scheme 7



would generate the metallacycle **4''**, which is identical to the starting complex **4**. Clearly such a mechanism involving sequential dissociation and reassociation of borane ligand would be nonproductive. However, dissociation of catecholborane followed by its addition across the C–C bond of the coordinated alkyne would be consistent with the kinetic data. This mechanism cannot be ruled out, but would be a highly unusual type of X–H addition process.

In an attempt to confirm the intramolecular reductive elimination mechanism, a crossover experiment was performed in which 4-methylcatecholborane was added to a solution of **4**, and the identity of the vinyl boronate ester product was determined. Instead of providing information on the mechanism of the vinyl boronate ester as designed, these experiments revealed a rapid borane dissociation from **4**. Both 4-methyl- and 4-*tert*-butyl-substituted vinyl boronate ester products and both 4-methyl- and 4-*tert*-butyl-substituted borane alkyne complexes were observed in solution. Further, borane exchange occurred faster than elimination of vinyl boronate ester product. A qualitative free energy diagram for the borane exchanges and intermolecular reductive elimination for the two alkyne complexes is presented in Figure 11. The two alkyne complexes coexist in equilibrium with a barrier to interconversion that is smaller than that for reductive elimination of the vinyl boronate ester products. As noted in the discussion of the spectroscopic features of **4**, this chemistry supports a structure of **4** that is a combination of a vinyl hydride and an alkyne borane complex.

Conclusion

Our studies on titanocene bisborane complexes demonstrate that catecholborane can behave as a simple two-electron-donating ligand. The stability of these complexes is attributed in part to the favorable match of the titanocene orbitals with the π -accepting orbitals of the borane ligand. The catecholborane ligand dissociates from the metal, and this dissociation allows

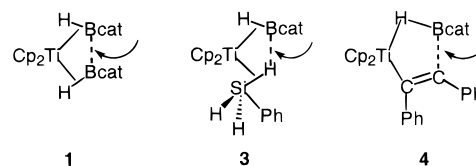


Figure 12. Stabilizing interactions in monoborane complexes.

for formation of new monoborane complexes $\text{Cp}_2\text{Ti}(\text{HBcat}')(\text{L})$ by coordination of L.

Although it is tempting to compare the stability of the different complexes $\text{Cp}_2\text{Ti}(\text{HBcat}')(\text{L})$ as a function of the nature of L, the stabilities of complexes **1**, **3**, and **4** are likely to be influenced by interactions that provide some degree of intramolecular interaction with boron as shown in Figure 12. A small boron–boron interaction in **1**, a substantial hydrogen–boron interaction in **3**, and a strong B–C interaction in **4** would complement the σ -coordination of the B–H bond to stabilize the compounds. Thus, a simple correlation can be made between the electronic nature of the ligand and the stability of the $\text{Cp}_2\text{Ti}(\text{HBcat}')(\text{L})$ complex only in the cases where L is CO or PMe_3 . In these cases, the stability of the monoborane σ -complex $\text{Cp}_2\text{Ti}(\text{HBcat}')(\text{L})$ appears to depend on the π -acidity and σ -basicity of the ligand L. The monoborane complex of the strong σ -donor $\text{Cp}_2\text{Ti}(\text{HBcat})(\text{PMe}_3)$ (**2b**) is generated by a comproportionation reaction between $\text{Cp}_2\text{Ti}(\text{PMe}_3)_2$ and $\text{Cp}_2\text{Ti}(\text{HBcat})_2$ and is stable in solution at 0 °C. The bisborane complex is less stable and decomposes more rapidly at 0 °C in the absence of added borane. Finally complex $\text{Cp}_2\text{Ti}(\text{HBcat}')(\text{CO})$ is merely a reactive intermediate in the CO substitution reactions. Attempts to prepare this compound by comproportionation between $\text{Cp}_2\text{Ti}(\text{CO})_2$ and $\text{Cp}_2\text{Ti}(\text{HBcat}')_2$ gave no reaction. Further, only $\text{Cp}_2\text{Ti}(\text{CO})_2$ and $\text{Cp}_2\text{Ti}(\text{HBcat}')_2$ were observed throughout the reaction of CO with $\text{Cp}_2\text{Ti}(\text{HBcat}')_2$ and when less than 2 equiv of CO was added to $\text{Cp}_2\text{Ti}(\text{HBcat}')_2$.

From the observed trend, it appears that π -acidic ligands such as carbon monoxide destabilize the σ -complex. Such ligands would compete with the borane for electron density on the metal that provides back-donation into boron and stabilizes the complex. Thus, the strong σ -donating and weak π -accepting ligand PMe_3 provides a more stable complex. This trend is supported by the electronic effects of substitution on the borane ligand. The rates for borane dissociation decreased with increased borane electrophilicity. Because ΔH and ΔH^\ddagger are closely related in dissociative substitution, the slower reaction of the complexes of electrophilic boranes is most likely due to their increased thermodynamic stability.

Experimental Section

General Considerations. Unless otherwise noted, all manipulations were conducted using standard Schlenk techniques or in an inert atmosphere glovebox. ^1H NMR spectra were obtained on a GE QE 300 MHz, GE Ω 300 MHz, or Bruker AM-500 MHz Fourier transform spectrometer. ^{11}B , ^{31}P , and ^2H NMR spectra were obtained on the Ω 300 MHz spectrometer operating at 96.38, 121.65, and 46.13 MHz, respectively. ^1H NMR spectra were recorded relative to residual protiated solvent. ^{11}B NMR and ^{31}P NMR spectra were recorded in units of parts per million relative to $\text{BH}_3\cdot\text{Et}_2\text{O}$ and 85% H_3PO_4 , respectively, as external standards.

Unless specified otherwise, all reagents were purchased from commercial suppliers and used without further purification. $\text{Cp}_2\text{Ti}(\text{PMe}_3)_2$,⁷⁰ Cp_2TiMe_2 ,⁷¹ $\text{Cp}_2\text{Ti}(\text{PhCCPh})$,⁷² $\text{Cp}_2\text{Ti}(\text{H}_2\text{SiPh}_2)(\text{PMe}_3)$,⁴⁴

(70) Kool, L. B.; Rausch, M. D.; Alt, H. G.; Herberhold, M.; Thewalt, U.; Wolf, B. *Angew. Chem., Int. Ed. Engl.* **1985**, *24*, 394.

(71) Erskine, G. H.; Wilson, D. A.; McCowan, J. D. *J. Organomet. Chem.* **1976**, *114*, 119.

4-chlorocatechol,⁷³ 4-methylthiocatechol,⁷⁴ and *B*-deuterio-4-methylcatecholborane⁷⁵ were prepared using literature procedures. All catechols were dried using a Dean–Stark apparatus prior to reaction. Protiated solvents were refluxed and distilled from purple solutions containing sodium benzophenone. Deuterated solvents were dried similarly, but were collected by vacuum transfer. Reaction yields that were obtained by ¹H NMR spectroscopy were determined using ferrocene as the internal standard.

Preparation of Catecholboranes. All the catecholboranes were prepared using a modification of a literature preparation for catecholborane (1,3,2-benzodioxaborole),⁷⁶ substituting BH₃·SMe₂ for BH₃·THF. To a stirred ether solution of the catechol was added BH₃·SMe₂ via syringe. Effervescence was observed, and the resulting clear tan-colored solution was stirred at room temperature for 4 h. Solvent was removed in vacuo, and the product was vacuum distilled at 0.5 Torr and 50–60 °C to give the catecholborane as a clear colorless oil.

4-*tert*-Butylcatecholborane. Product obtained in 62% yield (9.9 g). ¹H NMR (C₆D₆): δ 7.17 (d, *J* = 1.5 Hz, 1H), 6.94 (d, *J* = 8.4 Hz, 1H), 6.87 (dd, *J* = 8.4 Hz, 1.5 Hz, 1H), 4.40 (br q, *J*_{H–B} = 186 Hz, 1H), 1.15 (s, 9H). ¹¹B NMR (C₆D₆): δ 29.4 (d, *J*_{H–B} = 186 Hz). IR (Nujol, cm^{–1}): 2659 (s, ν_{H–B}), 1486 (s), 1431 (s), 1281 (s), 1250 (s), 1222 (s), 1130 (s), 866 (s), 812 (s).

4-Methylcatecholborane. Product obtained in 56% yield (3.0 g). ¹H NMR (C₆D₆): δ 6.86 (d, *J* = 8.2 Hz, 1H), 6.77 (s, 1H), 6.53 (d, *J* = 8.2 Hz, 1H), 4.0 (br q, *J*_{H–B} = 207 Hz, 1H), 2.02 (s, 3H). ¹¹B NMR (C₆D₆): δ 29.5 (d, *J*_{H–B} = 207 Hz). IR (Nujol, cm^{–1}): 2656 (s, ν_{H–B}), 1311 (s), 1281 (s), 1247 (s), 1168 (s), 1134 (s), 859 (s), 802 (s).

3,5-Di-*tert*-butylcatecholborane. Product obtained in 67% yield (3.2 g). ¹H NMR (C₆D₆): δ 7.19 (s, 1H), 7.15 (s, 1H), 4.3 (br q, *J*_{H–B} = 197 Hz, 1H), 1.461 (s, 9H), 1.223 (s, 9H). ¹¹B NMR (C₆D₆): δ 29.8 (d, *J*_{H–B} = 197 Hz). IR (Nujol, cm^{–1}): 2650 (s, ν_{H–B}), 1505 (s), 1402 (s), 1327 (s), 1232 (s), 1138 (s), 979 (s), 865 (s), 824 (s).

4-Chlorocatecholborane. Product obtained in 12% yield (129 mg). ¹H NMR (C₆D₆): δ 6.92 (d, *J* = 2.2 Hz, 1H), 6.71 (dd, *J* = 8.6, 2.2 Hz, 1H), 6.57 (d, *J* = 8.6, 197 Hz, 1H), 4.3 (br q, *J*_{H–B} = 197 Hz, 1H). ¹¹B NMR (C₆D₆): δ 30.2 (d, *J*_{H–B} = 197 Hz). IR (Nujol, cm^{–1}): 2661 (s, ν_{H–B}), 1276 (s), 1236 (s), 1157 (s), 1129 (s), 882 (s), 807 (s).

4-Methylthiocatecholborane. Product obtained in 44% yield (382 mg). ¹H NMR (C₆D₆): δ 7.03 (s, 1H), 6.79 (s, 1H), 6.79 (s, 1H), 4.5 (br q, *J*_{H–B} = 196 Hz, 1H), 1.916 (s, 3H). ¹¹B NMR (C₆D₆): δ 29.5 (d, *J*_{H–B} = 196 Hz). IR (Nujol, cm^{–1}): 2660 (s, ν_{H–B}), 1599 (s), 1422 (s), 1292 (s), 1272 (s), 1146 (s).

3-Fluorocatecholborane. Product obtained in 46.4% yield (2.54 g). ¹H NMR (C₆D₆): δ 6.61 (d, *J* = 7.2 Hz, 1H), 6.46–6.54 (m, 2H), 4.40 (br q, *J*_{H–B} = 205 Hz, 1H). ¹¹B NMR (C₆D₆): δ 29.2 (d, *J*_{H–B} = 205 Hz). IR (Nujol, cm^{–1}): 2664 (m, ν_{H–B}), 1634 (s), 1506 (s), 1338 (s), 1173 (s), 1023 (s), 873 (s), 766 (s).

Preparation of Titanocene Bisborane Complexes. All the titanocene bisborane complexes were prepared by adding the catecholborane to solutions of Cp₂TiMe₂ in 20 mL of pentane that were cooled in a –30 °C freezer. The resulting mixture was quickly placed back into the freezer (–30 °C) and left overnight. Pale yellow solids precipitated and were collected by vacuum filtration. The products were washed with cold pentane and then dried under reduced pressure.

Cp₂Ti(HBcat-4-*t*-Bu)₂ (1a). Yield: 63% (1.6 g). ¹H NMR (C₇D₈, –10 °C, two isomers): δ 7.05 (d, *J* = 2 Hz, 2H), 7.03 (d, 2 Hz, 2H), 6.87 (d, *J* = 7.8 Hz, 2H), 6.85 (d, *J* = 7.2 Hz, 2H), 6.58 (dd, *J* = 7 Hz, 2 Hz, 2H), 6.57 (dd, *J* = 8 Hz, 2 Hz, 2H), 5.48 (s, 5H), 5.46 (s, 10H), 5.44 (s, 5H), 1.10 (s, 18H), –5.67 (br s, 4H). ¹¹B NMR (C₇D₈, –10 °C): δ 46.0. IR (Nujol, cm^{–1}): 1722 (br, m), 1603 (s), 1493 (s), 1423 (s), 1255 (s), 861 (s), 828 (s).

Cp₂Ti(HBcat-3,5-di-*t*-Bu)₂ (1b). Yield: 74% (394 mg). ¹H NMR (C₇D₈, –10 °C): (C₂ isomer) δ 6.95 (d, *J* = 1.5 Hz, 2H), 6.81 (d, *J* =

1.5 Hz, 2H), 5.42 (s, 10H), 1.66 (s, 18H), 1.12 (s, 18H), –6.15 (br s, 2H). (C₅ isomer) δ 6.92 (s, 2H), 6.73 (s, 2H), 5.46 (s, 5H), 5.42 (s, 5H), 1.58 (s, 18H), 1.21 (s, 18H), –5.37 (br s, 2H). ¹¹B NMR (C₇D₈, –10 °C): δ 46.3. IR (Nujol, cm^{–1}): 1665 (br, m), 1621 (m), 1592 (s), 1512 (s), 1408 (s), 1287 (s), 1072 (s), 828 (s), 758 (s).

Cp₂Ti(HBcat-4-Me)₂ (1c). Yield: 83% (833 mg). ¹H NMR (C₇D₈, –10 °C, two isomers): δ 6.85 (dd, *J* = 8.0, 4.1 Hz, 4H), 6.76 (d, *J* = 4.1 Hz, 4H), 6.35 (d, *J* = 8.0, 4H), 5.42 (s, 5H), 5.41 (s, 10H), 5.40 (s, 5H), 1.97 (s, 6H), 1.96 (s, 6H), –5.45 (br s, 4H). ¹¹B NMR (C₇D₈, –10 °C): δ 45.8. IR (Nujol, cm^{–1}): 1650 (br, m), 1611 (m), 1481 (s), 1431 (s), 1234 (s), 1101 (s), 1099 (s), 1000 (s), 828 (s), 750 (s).

Cp₂Ti(HBcat-4-Cl)₂ (1d). Yield: 67% (49.0 mg). ¹H NMR (C₇D₈, –10 °C, two isomers): δ 6.95 (d, *J* = 1.6 Hz, 2H), 6.94 (d, *J* = 1.6 Hz, 2H), 6.62 (d, *J* = 5.4 Hz, 2H), 6.59 (d, *J* = 5.412, 2H), 6.50 (dd, *J* = 5.4 Hz, 1.6 Hz, 2H), 6.48 (dd, *J* = 4.7 Hz, 2.3 Hz, 2H), 5.30 (s, 5H), 5.30 (s, 10H), 5.29 (s, 5H), –5.80 (br s, 4H). ¹¹B NMR (C₇D₈, –10 °C): δ 45.8. IR (Nujol, cm^{–1}): 1695 (br, m), 1599 (m), 1477 (br), 1232 (s), 1210 (s), 1113 (s), 825 (s).

Cp₂Ti(HBcat-4-SMe)₂ (1e). Yield: 29% (90 mg). ¹H NMR (C₇D₈, –10 °C, two isomers): δ 6.78 (d, *J* = 3.6 Hz, 2H), 6.75 (d, *J* = 3.6 Hz, 2H), 6.57 (d, *J* = 7.7 Hz, 2H), 6.54 (d, *J* = 7.7 Hz, 2H), 5.40 (s, 5H), 5.39 (s, 10H), 5.38 (s, 5H), –5.83 (br s, 4H), the most downfield aromatic resonance was obscured by the residual protiated toluene solvent. ¹¹B NMR (C₇D₈, –10 °C): δ 45.7. IR (Nujol, cm^{–1}): 1651 (br, m), 1599 (m), 1231 (s), 1078 (s), 880 (s).

Cp₂Ti(HBcat-3-F)₂ (1f). Yield: 76.5% (168 mg). ¹H NMR (C₇D₈, –10 °C, two isomers): δ 6.62 (m, 4H), 6.49 (m, 4H), 6.32 (m, 4H), 5.33 (s, 5H), 5.33 (s, 10H), 5.313 (s, 5H), –5.8 (br s, 4H). ¹¹B NMR (C₇D₈, –10 °C): δ 45.7. IR (Nujol, cm^{–1}): 1672 (br, m), 1626 (m), 1492 (s), 1435 (s), 1270 (s), 1232 (s), 1048 (m), 1002 (s), 849 (s), 769 (s), 723 (s).

Cp₂Ti(HBcat)₂ (1g). Yield: 94% (1.77 g). Due to the insolubility of **1g** in aromatic solvents, NMR data were obtained by reacting a solution of Cp₂TiMe₂ (2.0 mg, 0.0097 mmol) in toluene-*d*₈ with catecholborane (3.8 mg, 0.031 mmol) in an NMR tube at –10 °C and obtaining NMR data prior to the precipitation of **1g** from solution. ¹H NMR (C₇D₈, –10 °C): δ 6.95 (m, 4H), 6.57 (m, 4H), 5.40 (s, 10H), –5.85 (br s, 2H). ¹¹B NMR (C₇D₈, –10 °C): δ 45.0. IR (Nujol, cm^{–1}): 1683 (br, m), 1612 (m), 1485 (s), 1459 (s), 1249 (s), 1217 (s), 1130 (s), 1027 (s), 823 (s), 803 (s).

Cp₂Ti(DBcat)₂ (1g-*d*₂). Yield: 58% (333 mg). Due to the insolubility of **1g-d**₂ in aromatic solvents, NMR data were obtained by reacting a solution of Cp₂TiMe₂ (2.0 mg, 0.0097 mmol) in toluene with *B*-deuteriocatecholborane (3.7 mg, 0.031 mmol) in an NMR tube at –10 °C and obtaining NMR data prior to the precipitation of **1g-d**₂ from solution. ²H NMR (C₇H₈, –10 °C): δ –5.9. ¹¹B NMR (C₇H₈, –10 °C): δ 45.0. IR (Nujol, cm^{–1}): 1238 (s), 1193 (s), 1105 (m), 1032 (m), 985 (s), 865 (m), 826 (s), 749 (s).

Generation of Cp₂Ti(HBcat-4-*t*-Bu)(PMe₃) (2a) in Situ. Into an NMR tube were weighed **1a** (10.0 mg, 0.0189 mmol) and ferrocene (approximately 3 mg). The tube was sealed with a septum and immersed in a dry ice–acetone bath. To the tube was added 0.6 mL of toluene-*d*₈, and a ¹H NMR spectrum was obtained at 0 °C. The tube was immersed again in the dry ice–acetone bath, and PMe₃ (1.96 μL, 0.0189 mmol) was added by syringe. The tube was shaken and allowed to remain at 0 °C for 3 h. A ¹H NMR spectrum at 0 °C indicated that **2a** was formed in 84% yield. ¹H NMR (C₇D₈, 0 °C): δ 7.18 (d, *J* = 1.7 Hz, 1H), 6.86 (d, *J* = 8.5 Hz, 1H), 6.79 (dd, *J* = 8.5, 1.7 Hz, 1H), 5.03 (d, *J*_{H–P} = 2.7 Hz, 5H), 5.01 (d, *J*_{H–P} = 2.7 Hz, 5H), 1.26 (s, 9H), 0.75 (d, *J* = 6.0 Hz, 9H), –9.7 (br s, 1H). ¹¹B NMR (C₇D₈, 0 °C): δ 64.0. ³¹P{¹H} NMR: δ 29.3.

Preparation of Cp₂Ti(HBcat)(PMe₃) (2b). Into a side-arm flask were weighed Cp₂Ti(PMe₃)₂ (395 mg, 1.20 mmol) and **1g** (500 mg, 0.947 mmol). The flask was cooled to –30 °C and then charged with 3 mL of cold (–30 °C) toluene. This solution was stirred for 90 min at 0 °C. The resulting dark maroon solution was then kept at –30 °C for 2 d, after which time a dark pink solid precipitated from solution. The dark maroon supernatant was removed, and the solid was dried in vacuo to give 413 mg (46.4%) of Cp₂Ti(HBcat)(PMe₃). ¹H NMR (C₇D₈, 0 °C): δ 7.09 (m, 2H), 6.79 (m, 2H), 5.02 (d, *J*_{H–P} = 3.0 Hz, 10H), 0.75 (d, *J*_{H–P} = 6.3 Hz, 9H), –9.8 (br s, 1H). ¹¹B NMR (C₇D₈, 0 °C):

(72) Shur, V. B.; Burlakov, V. V.; Vol'pin, M. E. *J. Organomet. Chem.* **1988**, *347*, 77.

(73) Kabalka, G. W.; Reddy, N. K.; Narayana, C. *Tetrahedron Lett.* **1992**, *33*, 865.

(74) Cooksey, C., J.; Land, E. J.; Riley, P. A. *Org. Prep. Proced. Int.* **1996**, *28*, 463.

(75) Männig, D.; Nöth, H. *J. Chem. Soc., Dalton Trans.* **1985**, 1689.

(76) Brown, H. C.; Gupta, S. K. *J. Am. Chem. Soc.* **1971**, *93*, 1816.

δ 64.2. $^{31}\text{P}\{^1\text{H}\}$ NMR (C_7D_8 , 0 °C): δ 29.3. $^{13}\text{C}\{^1\text{H}\}$ NMR (C_7D_8 , -5 °C): δ 153.09, 120.69, 110.10, 96.69, 20.37 (this resonance is obscured by toluene, but was identified by a ^1H - ^{13}C correlation experiment; the coupling constant was not determined). IR (Nujol, cm^{-1}): 1650 (br, m), 1485 (s), 1426 (s), 1355 (s), 1237 (s), 1207 (s), 1004 (s), 960 (s), 846 (s), 806 (s).

Preparation of $\text{Cp}_2\text{Ti}(\text{HBcat-3-F})(\text{PMe}_3)$ (2c**).** Compound **2c** was prepared in 40% yield (13.7 mg) using a procedure similar to that for the preparation of **2b**. ^1H NMR (C_7D_8 , 0 °C): δ 6.75 (m, 1H), 6.53 (m, 2H), 4.97 (d, $J_{\text{H-P}} = 3.0$ Hz, 10H), 0.70 (d, $J_{\text{H-P}} = 6.3$ Hz, 9H), -9.4 (br s, 1H). ^{11}B NMR (C_7D_8 , 0 °C): δ 64.9. $^{31}\text{P}\{^1\text{H}\}$ NMR (C_7D_8 , 0 °C): δ 27.9.

Preparation of $\text{Cp}_2\text{Ti}(\text{PhSiH}_3)(\text{HBcat}')$ (3**); $\text{HBcat}' = \text{HBO}_2\text{C}_6\text{H}_3\text{-4-}t\text{-Bu}$.** A side-arm flask was charged with **1a** (300 mg, 0.568 mmol), sealed with a septum, and cooled to -78 °C. Approximately 10 mL of toluene was then added to the flask via syringe. With stirring, the yellow slurry was allowed to warm to -5 °C, and phenylsilane (100 μL , 0.810 mmol) was added to the mixture by syringe. Stirring was continued for 6 h, over which time the solution became yellow-green. Solvent was completely removed from the mixture under vacuum at -5 °C to afford a yellow powder. The product was collected by vacuum filtration, washed with cold pentane, and dried under vacuum (103.4 mg, 39%). ^1H NMR (C_7D_8 , -80 °C): 7.68 (d, $J = 6.3$ Hz, 2H), 7.29 (s, 1H), 7.14 (m, 3H), 7.19 (d, $J = 7.8$ Hz, 1H), 6.79 (d, $J = 7.8$ Hz, 1H), 5.13 (br s, 1H), 5.11 (br s, 1H), 4.99 (s, 5H), 4.94 (s, 5H), 1.29 (s, 9H), -4.99 (br s, 1H), -6.78 (br s, 1H). ^{11}B NMR (C_7D_8 , 0 °C): 37.1. IR (Nujol, cm^{-1}): 2066 (s), 1739 (s), 1773 (s), 1252 (s), 1213 (s), 1024 (s), 800 (s).

Preparation of $\text{Cp}_2\text{Ti}(\text{PhSiH}_3)(\text{DBcat}')$. This compound was prepared in 74% yield (214.7 mg) using the method described for the synthesis of **3** and DBcat' . ^2H NMR: δ -6.78, -4.98, 4.90. ^{11}B NMR: δ 37.0. IR (Nujol, cm^{-1}): 2093 (s), 2053 (s), 1556 (s), 1466 (s), 1380 (m), 1299 (m), 1220 (m), 1100 (s), 780 (s), 600 (s).

Generation of $\text{Cp}_2\text{Ti}(\text{PhCCPh})(\text{HBcat}')$ (4**); $\text{HBcat}' = \text{HBO}_2\text{C}_6\text{H}_3\text{-4-}t\text{-Bu}$ in Situ.** A solution of $\text{Cp}_2\text{Ti}(\text{PhCCPh})$ (5.0 mg, 0.014 mmol) in approximately 0.6 mL of toluene- d_8 was placed into an NMR tube, and the tube was sealed with a septum. The tube was cooled to -78 °C, and 4-*tert*-butylcatecholborane (2.5 μL , 0.014 mmol) was added by syringe. The tube was then quickly introduced into the precooled probe of the NMR spectrometer for analysis. ^1H NMR (C_7D_8 , -60 °C): δ 7.07 (m, 6H), 7.03 (d, $J = 1.9$ Hz, 1H), 6.89 (d, $J = 8.1$ Hz, 1H), 6.83 (m, 4H), 6.67 (dd, $J = 8.1, 1.9$ Hz, 1H), 5.44 (s, 5H), 5.43 (s, 5H), 1.25 (s, 9H), -1.59 (br s, 1H). ^{11}B NMR (C_7D_8 , -30 °C): δ 29.8. $^{13}\text{C}\{^1\text{H}\}$ NMR (C_7D_8 , -60 °C): δ 207.7, 153.8, 151.8, 141.9, 141.1, 140.1, 129.8, 128.6, 127.9, 126.2, 115.9, 107.9, 34.5, 31.8. (five aromatic carbons are obscured by toluene solvent).

Reaction of **1c with *B*-Deuterio-4-methylcatecholborane.** Into an NMR tube was weighed 10 mg (0.022 mmol) of **1c**, and the tube was sealed with a septum. The tube was cooled to -78 °C, and a solution of *B*-deuterio-4-methylcatecholborane (31.6 mg, 0.22 mmol) in 0.6 mL of toluene was added into the tube by syringe. The tube was quickly immersed into the precooled probe (-5 °C) of the NMR spectrometer for analysis. Spectroscopic analyses of **1c-d**₂: ^{11}B NMR (-5 °C, C_7H_8) δ 46; ^2H NMR (-5 °C, C_7H_8) δ -5.5.

Reaction of **1c with Catecholborane.** Into a vial were weighed 10 mg (0.022 mmol) of **1c** and 1 equiv of ferrocene as an internal standard. Catecholborane (52 mg, 0.44 mmol) in 0.6 mL of toluene- d_8 was added into the tube by syringe. A yellow solid (**1g**) was deposited. A ^1H NMR spectrum was obtained of the supernatant to determine the yield of extruded 4-methylcatecholborane.

Ligand Substitution Reactions of **2b.** Into an NMR tube was weighed 10 mg (0.027 mmol) of **2b**, and the tube was sealed with a septum. The tube was cooled to -78 °C, and a solution of reagent in 0.6 mL of toluene- d_8 was added into the tube by syringe. The tube was quickly immersed into the precooled probe (-5 °C) of the NMR spectrometer for analysis. Experiments were performed using trimethylphosphine- d_9 , *B*-deuteriocatecholborane, and 3-fluorocatecholborane as reagents to give $\text{Cp}_2\text{Ti}(\text{HBcat})(\text{PMe}_3\text{-}d_9)$, $\text{Cp}_2\text{Ti}(\text{DBcat})(\text{PMe}_3)$, and **2c**, respectively. Spectroscopic analyses are as follows. $\text{Cp}_2\text{Ti}(\text{HBcat})(\text{PMe}_3\text{-}d_9)$: ^{11}B NMR (-5 °C, C_7H_8) δ 64; ^2H NMR (-5 °C, C_7H_8) δ 0.80; ^{31}P NMR (-5 °C, C_7H_8) δ 26.5. $\text{Cp}_2\text{Ti}(\text{DBcat})(\text{PMe}_3)$: ^{11}B NMR

(-5 °C, C_7H_8) δ 64; ^2H NMR (-5 °C, C_7H_8) δ -9.9; IR (Nujol, cm^{-1}) 1591 (s), 1485 (s), 1426 (s), 1349 (m), 1237 (m), 1207 (m), 1184 (br, m), 950 (m), 800 (s).

Reaction of **2b with Phenylsilane.** Into an NMR tube was weighed 9.6 mg (0.026 mmol) of **2b**, and the tube was sealed with a septum. The tube was cooled to -78 °C, and a solution of phenylsilane (0.26 mmol, 48 mg) in 0.6 mL of toluene- d_8 was added to the tube by syringe. The tube was quickly immersed into the precooled probe (-5 °C) of the NMR spectrometer for analysis.

Reaction of $\text{Cp}_2\text{Ti}(\text{H}_2\text{SiPh}_2)(\text{PMe}_3)$ with HBcat. Into an NMR tube was weighed 20 mg (0.046 mmol) of $\text{Cp}_2\text{Ti}(\text{H}_2\text{SiPh}_2)(\text{PMe}_3)$. The tube was sealed with a septum. The tube was cooled to -78 °C, and a solution of diphenylsilane (85 mg, 0.46 mmol) in 0.4 mL of toluene- d_8 was added by syringe. A solution of catecholborane (5.5 mg, 0.046 mmol) in 0.2 mL of toluene- d_8 was then added. The tube was quickly immersed into the precooled probe (-5 °C) of the NMR spectrometer for analysis.

Kinetic Studies of the Reaction of PMe_3 with **1a-e.** Into an NMR tube was weighed 0.0057 mmol of the appropriate titanocene borane σ -complex, and the tube was sealed with a septum. The NMR tube was then cooled to -78 °C by immersing it into a dry ice-acetone bath, and 0.6 mL of toluene- d_8 was added to the NMR tube by syringe. The tube was shaken to dissolve all of the solid without allowing the sample to warm. The tube was then reimmersed into the dry ice-acetone bath, and 1 equiv of PMe_3 was added by syringe. The tube was quickly shaken and introduced into the precooled (-30 °C) probe of the NMR spectrometer. Single-pulse experiments were performed every 90 s over at least 3 half-lives using an automated program. The experiment was repeated at -15, -20, -25, -35, and -40 °C for values of the rate constants to be used in the Eyring plot. Rate measurements were performed by measuring the integrals of the cyclopentadienyl peaks of the titanocene starting material and product by ^1H NMR spectroscopy at -30 °C. For studies of the dependence of the reaction rate on HBcat' and PMe_3 concentrations, the appropriate amounts of phosphine and 4-*tert*-butylcatecholborane were added by syringe to an NMR tube containing 0.0057 mmol of **1a** before the tube was introduced into the NMR spectrometer. Measurements were made with 0.0945 mmol (5 equiv) of added 4-*tert*-butylcatecholborane and 0.0284, 0.0471, and 0.0853 mmol of added PMe_3 . Measurements were also made with 0.0341 mmol (6 equiv) of PMe_3 and 0.0170, 0.0341, and 0.0517 mmol of added 4-*tert*-butylcatecholborane.

Reaction of **1a with CO.** Into a vial was weighed 3.0 mg (0.0057 mmol) of **1a**. The vial was cooled to -30 °C. To this vial was added 0.6 mL of cold toluene- d_8 , and the resulting yellow solution was kept at -30 °C for 5 min. The solution was then quickly transferred to an NMR pressure tube, and the tube was sealed. The tube was returned to the freezer for another 5 min, after which time it was rapidly removed from the drybox and fully immersed into a Dewar flask containing a dry ice-acetone mixture. The tube was then connected to a tank of carbon monoxide using a Swage-lock adapter without removing it from the dry ice-acetone bath. One atm of CO gas was added to the tube, and the tube was sealed again. The tube was then shaken and rapidly introduced into the precooled NMR spectrometer. Rate measurements were made by monitoring the Cp resonances in **1a** and the product, $\text{Cp}_2\text{Ti}(\text{CO})_2$. The experiment was repeated with 3 atm of CO gas to study the dependence of the reaction rate on CO concentration. Single-pulse experiments were performed every 90 s over at least 3 half-lives at -30 °C.

Reaction of **1a with PhSiH_3 .** Into an NMR tube was weighed 3.0 mg (0.0057 mmol) of **1a**, and the tube was sealed with a septum. The NMR tube was then cooled to -78 °C by fully immersing it into a dry ice-acetone bath, and 0.6 mL of toluene- d_8 was added to the NMR tube by syringe. The tube was shaken to dissolve all of the solid without allowing it to warm. The tube was then reimmersed into the dry ice-acetone bath, and 1.4 μL (0.011 mmol) of PhSiH_3 was added by syringe. The tube was quickly shaken and introduced into the precooled (-30 °C) probe of the NMR spectrometer. Rate measurements were performed by monitoring the integrals of the cyclopentadienyl peaks of the titanocene starting material and product by ^1H NMR spectroscopy at -30 °C. Single-pulse experiments were performed every 90 s over at least 3 half-lives.

Reaction of PhCCPh with 1a. Into an NMR tube were weighed 3.0 mg (0.0057 mmol) of **1a** and 3.0 mg (0.017 mmol) of diphenylacetylene, and the tube was sealed with a septum. The NMR tube was then cooled to $-78\text{ }^{\circ}\text{C}$ by fully immersing it into a dry ice–acetone bath, and 0.6 mL of toluene- d_8 was added to the NMR tube by syringe. The tube was shaken to dissolve all of the solid without allowing it to warm. The NMR tube was introduced into the precooled ($-30\text{ }^{\circ}\text{C}$) probe of the NMR spectrometer. Rate measurements were performed by monitoring the integrals of the cyclopentadienyl peaks of the titanocene starting material and product by ^1H NMR spectroscopy at $-30\text{ }^{\circ}\text{C}$. Single-pulse experiments were performed every 90 s over at least 3 half-lives.

Kinetic Studies of the Formation of Vinyl Boronate Ester from 4. Into a vial was weighed 5.0 mg (0.014 mmol) of $\text{Cp}_2\text{Ti}(\text{PhCCPh})$, and 0.5 mL of toluene- d_8 was added. The solution was transferred to an NMR tube, and the tube was sealed with a septum. The solution was then immersed into a dry ice–acetone mixture and allowed to cool. To the NMR tube was then added 0.042 mmol of the appropriate catecholborane by syringe. The tube was rapidly shaken and introduced into the precooled probe ($-30\text{ }^{\circ}\text{C}$) of the NMR spectrometer. Rate measurements were performed by monitoring the integrals of the vinylic protons of the vinyl boronate ester product. Single-pulse experiments were performed every 90 s over at least 3 half-lives.

Crystallographic Analysis of 1g. Pale yellow single crystals of **1g** that were suitable for X-ray diffraction studies were obtained by cooling a highly dilute solution of Cp_2TiMe_2 and catecholborane to $-30\text{ }^{\circ}\text{C}$ for several days. The X-ray intensity data were measured at 195 K with graphite monochromatic Mo $K\alpha$ radiation. Crystal data are provided in Tables 1 and 2. For $Z = 2$ and $\text{FW} = 510.06$, the calculated density is 1.361 g/cm^3 . The space group was determined to be $P2_1/m$ (no. 11). The structure was solved by direct methods using the SHELXS software package. The non-hydrogen atoms were refined anisotropically. The hydrogen atoms were observed in the difference map, and H1 was isotropically refined. The hydrogens are included in idealized positions, except for H1 which was included in the difference map position. The final cycle of full matrix least squares refinement was based on 1552 observed reflections ($I > 3.00\sigma(I)$) and 178 variable parameters and converged (largest parameter shift was 0.00 times its esd) with

unweighted and weighted agreement factors of $R = 5.7\%$ and $R_w = 6.4\%$. The crystallographic data for **1g** were deposited in the Cambridge Crystallographic Data Centre under reference code TUBSUE as part of a previous communication.³⁹

Crystallographic Analysis of 2c. Dark red prism-like single crystals of **2c** that were suitable for X-ray diffraction studies were obtained by cooling a concentrated toluene solution of **2c** to $-30\text{ }^{\circ}\text{C}$ for several days. X-ray data for **2c** were measured at 153 K with a Mo-target X-ray tube ($\lambda = 0.71073\text{ \AA}$). Crystal data are provided in Tables 3 and 4. A total of 1321 frames were collected with a scan width of 0.3° in ω and an exposure time of 30 s/frame. The frames were integrated with the Siemens SAINT software package using a narrow-frame integration algorithm. The integration of the data using a triclinic unit cell yielded a total of 5507 reflections to a maximum 2θ angle of 45° , 2329 of which were independent and 1943 of which were greater than $4\sigma(F)$. The final cell constants are based upon the refinement of the XYZ-centroids of 3685 reflections above $2\sigma(I)$. The data were corrected for absorption using the SADABS program with minimum and maximum transmission coefficients of 0.564 and 0.928, respectively. The structure was solved and refined using the Siemens SHELXTL (version 5.0) software package, using space group $P\bar{1}$, with $Z = 2$. Final anisotropic full-matrix least-squares refinement on F^2 converged at $R1 = 6.38\%$, $wR^2 = 16.31\%$, and a goodness of fit of 1.024. The hydrogen atoms were located and refined. The crystallographic data for **2c** were deposited in the Cambridge Crystallographic Data Centre with code CCDC-100125 as part of a previous communication.⁴⁰

Acknowledgment. This work was supported by the National Science Foundation. We thank the Dreyfus Foundation for a Camille Dreyfus Teacher-Scholar Award. J.F.H. is an Alfred P. Sloan Research Fellow. In addition, we thank Susan De Gala for the X-ray structural analysis of **1g** and Charles Campana at Siemens for the X-ray analysis of **2c**. We are grateful to Odile Eisenstein for her insightful analysis on several aspects of this work.

JA9900757